Eidgenössische Technische Hochschule Zürich

Ecole polytechnique fédérale de Zurich
Politecnico federale di Zurigo
Swiss Federal Institute of Technology Zurich

Convergence analysis of Finite Element Methods for $H(\mathrm{div};\Omega)$-elliptic interface problems

R. Hiptmair, J. Li and J. Zou*

Research Report No. 2010-14
May 2010

Seminar für Angewandte Mathematik
Eidgenössische Technische Hochschule
CH-8092 Zürich
Switzerland

*Department of Mathematics, The Chinese University of Hong Kong, Shatin, N.T., Hong Kong. The work of this author was substantially supported by Hong Kong RGC grants (Projects 404407 and 404606).

Convergence Analysis of Finite Element Methods for $\boldsymbol{H}(\mathrm{div};\Omega)$-Elliptic Interface Problems

Ralf Hiptmair* Jingzhi Li† Jun Zou‡

May 10, 2010

Abstract

In this article we analyze a finite element method for solving $\boldsymbol{H}(\mathrm{div};\Omega)$-elliptic interface problems in general three-dimensional Lipschitz domains with smooth material interfaces. The continuous problems are discretized by means of lowest order $\boldsymbol{H}(\mathrm{div};\Omega)$-conforming finite elements of the first family (Raviart-Thomas or Nédélec face elements) on a family of unstructured oriented tetrahedral meshes. These resolve the smooth interface in the sense of sufficient approximation in terms of a parameter δ that quantifies the mismatch between the smooth interface and the finite element mesh. Optimal error estimates in the $\boldsymbol{H}(\mathrm{div};\Omega)$-norms are obtained for the first time. The analysis is based on a so-called δ-strip argument, a new extension theorem for $\boldsymbol{H}^1(\mathrm{div})$-functions across smooth interfaces, a novel non-standard interface-aware interpolation operator, and a perturbation argument for degrees of freedom in $\boldsymbol{H}(\mathrm{div};\Omega)$-conforming finite elements. Numerical tests are presented to verify the theoretical predictions and confirm the optimal order convergence of the numerical solution.

Key words. $\boldsymbol{H}(\mathrm{div};\Omega)$-elliptic interface problems, finite element methods, face elements, convergence analysis.

AMS subject classification 2000. 65N12, 65N30

1 Introduction

Given a bounded domain $\Omega \subset \mathbb{R}^3$ with a Lipschitz boundary, we assume that the domain Ω consists of two subdomains Ω_1 and Ω_2, where $\Omega_1 \subset\subset \Omega, \Omega_2 := \Omega \setminus \overline{\Omega}_1$. The internal interface $\Gamma := \partial\Omega_1$ is assumed to be sufficiently *smooth*, namely, at least C^2-smooth (see Figure 1 for an illustration of the geometric setting). We are concerned with solving the $\boldsymbol{H}(\mathrm{div};\Omega)$-elliptic interface problem

$$-\mathbf{grad}(\chi \,\mathrm{div}\,\mathbf{u}) + \beta\mathbf{u} = \mathbf{f} \quad \text{in } \Omega\,, \tag{1.1}$$

with Dirichlet boundary condition

$$\mathbf{u}\cdot\mathbf{n} = 0 \quad \text{on } \partial\Omega\,, \tag{1.2}$$

and jump conditions on the interface

$$[\mathbf{n}\cdot\mathbf{u}] = 0 \quad \text{on } \Gamma\,, \tag{1.3}$$

$$[\chi \,\mathrm{div}\,\mathbf{u}] = 0 \quad \text{on } \Gamma\,, \tag{1.4}$$

*SAM, ETH, Zürich, CH-8092 Zürich, Switzerland (hiptmair@sam.math.ethz.ch).

†SAM, ETH, Zürich, CH-8092 Zürich, Switzerland (jingzhi.li@sam.math.ethz.ch).

‡Department of Mathematics, The Chinese University of Hong Kong, Shatin, N.T., Hong Kong. The work of this author was substantially supported by Hong Kong RGC grants (Project 404407 and 404606). (zou@math.cuhk.edu.hk).

where $\mathbf{f} \in \boldsymbol{L}^2(\Omega)$ is the source term, and $\mathbf{n}$ stands for a unit normal vector to the boundary $\partial\Omega_1$ pointing into Ω_2. By $[\mathbf{v}] := \mathbf{v}_1 - \mathbf{v}_2$ we denote the jump of a function $\mathbf{v}$ across the interface Γ. For ease of exposition, we assume that the coefficient functions χ and β are piecewise constant, i.e.

$$\chi(\mathbf{x}) = \begin{cases} \chi_1, & \mathbf{x} \in \Omega_1; \\ \chi_2, & \mathbf{x} \in \Omega_2, \end{cases} \qquad \beta(\mathbf{x}) = \begin{cases} \beta_1, & \mathbf{x} \in \Omega_1; \\ \beta_2, & \mathbf{x} \in \Omega_2, \end{cases}$$

where χ_i's and β_i's ($i = 1, 2$) are positive constants. The more general case of piecewise smooth uniformly positive coefficients in $L^\infty(\Omega)$ can be treated similarly with no essential difficulty by using techniques like local averaging in an element.

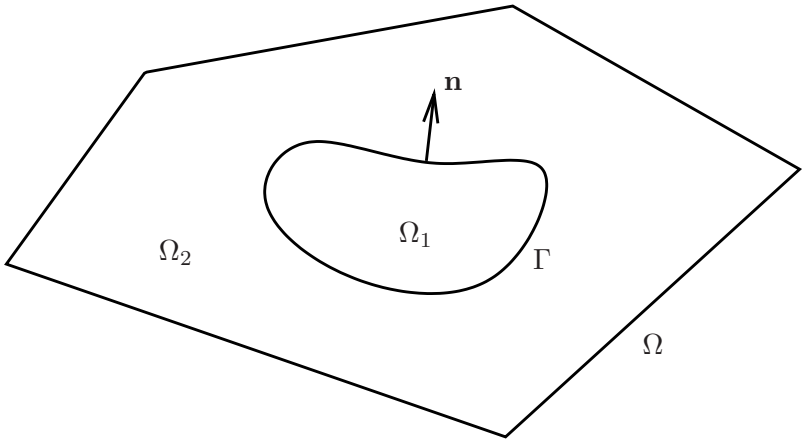

Figure 1: An illustrative sketch of the setting of the problem.

$\boldsymbol{H}(\mathrm{div};\Omega)$-elliptic interface problems like (1.1)–(1.4) arise from, e.g., the first-order system least-squares formulation of elliptic interface problem, or preconditioning for the mixed finite element using a gradient formulation of the Dirichlet problem (see, e.g., [2,7,12,17,26] and the references therein). Finite element methods for $\boldsymbol{H}(\mathrm{div};\Omega)$-elliptic problems have been well studied in [2,14,17]. Nevertheless, the discontinuity of the coefficients across the smooth interface creates additional challenges. First, the global regularity of the solution might be significantly lower than the local regularity in each subdomain due to the jump of coefficients across the interface. Thus, the techniques used for traditional $\boldsymbol{H}(\mathrm{div};\Omega)$-finite element methods with full regularity are not applicable here. Second, we are confronted with the issues of how to approximate the smooth interface by the finite element mesh, how to define practical numerical quadrature for those elements partially cut through by the interface, and, last but not least, whether it is still possible to obtain optimal convergence order using the $\boldsymbol{H}(\mathrm{div};\Omega)$-conforming finite element method for $\boldsymbol{H}(\mathrm{div};\Omega)$-elliptic interface problems? Below we address all these issues.

Due to the practical relevance of interface problems in many engineering and industrial applications, numerical solution methods for interface problems have been investigated extensively. One may refer to the monograph [20] and the references therein for a history of the development in this research field. Numerous variants of finite element methods (FEMs) for classical elliptic interface problems in $H^1(\Omega)$- and $\boldsymbol{H}(\mathbf{curl};\Omega)$-settings have been extensively studied in the past few decades. Interested readers may refer to [3,4,6,9,13,16,18,19,24]. Nevertheless, to the best knowledge of the authors, there seems to exist no corresponding work on the convergence analysis of $\boldsymbol{H}(\mathrm{div};\Omega)$-elliptic interface problems discretized by means of interface-aligned face elements.

This article completes the numerical analysis of conforming finite element methods for three important classes of elliptic interface problems, namely those set in $H^1(\Omega)$, $\boldsymbol{H}(\mathbf{curl};\Omega)$ and $\boldsymbol{H}(\mathrm{div};\Omega)$. General higher order Lagrange finite element methods for $H^1(\Omega)$-elliptic interface problems were discussed in [19]. In this paper key tools and concepts like the δ-strip argument and the perturbed interpolation were first introduced. A crucial insight obtained in [19] was that the optimal convergence order depends not only on the mesh size but also on the mismatch between the interface and the mesh. Subsequently, in [16] we investigated $\boldsymbol{H}(\mathbf{curl};\Omega)$-elliptic interface problems using lowest order edge elements of the first family. We derived optimal order convergence in the

$\boldsymbol{H}(\mathbf{curl};\Omega)$-norm for the first time. We relied on novel techniques such as the generalization of the concept of perturbed interpolation to edge elements, an $\boldsymbol{H}^1(\mathbf{curl};\Omega_i)$ extension theorem and what we dubbed a "pyramid argument".

The main contribution of the current work is to derive optimal order convergence in the $\boldsymbol{H}(\mathrm{div};\Omega)$-norm for $\boldsymbol{H}(\mathrm{div};\Omega)$-elliptic interface problems using lowest order Raviart-Thomas (or Nédélec) $\boldsymbol{H}(\mathrm{div};\Omega)$-conforming finite elements [5,22]. We follow the lines of [16], with new twists, entailed by the "more non-local" nature of the degrees of freedom for $\boldsymbol{H}(\mathrm{div};\Omega)$-conforming (face) finite elements. Therefore, the analytical tools and techniques had to be adjusted. This led to

- a new non-standard interface-aware face element based interpolant, which is shown to possess optimal approximation in the sense of the $\boldsymbol{H}(\mathrm{div};\Omega)$-norm, Sect. 2.4,
- a modified δ-strip argument for quantifying the relation of error estimate near the interface in terms of the mismatch parameter δ between the triangulation and the smooth interface, see Cor. 3.2,
- a new extension theorem for $\boldsymbol{H}^1(\mathrm{div};\Omega_i)$ functions across smooth interfaces for $i = 1, 2$, which bridges the gap between standard and non-standard interpolation and thus is crucial for the convergence analysis, see Thm. 3.4,
- a perturbation argument for the degrees of freedom of $\boldsymbol{H}(\mathrm{div};\Omega)$-conforming finite elements, see the proof of the pivotal Lemma 4.2.

The remainder of the paper is organized as follows: In Section 2, we first introduce some necessary notations and assumptions to be used later, then derive the variational formulation for the $\boldsymbol{H}(\mathrm{div};\Omega)$-elliptic interface problem, and propose a practical finite element approximation using the lowest order Raviart-Thomas finite element spaces. In Section 3 we establish some important auxiliary results, including a δ-strip argument for error estimation near the interface and the construction of a new extension operator for $\boldsymbol{H}^1(\mathrm{div};\Omega_i)$ functions across smooth interfaces for $i = 1, 2$. In Section 4, we prove optimal order convergence in the sense of $\boldsymbol{H}(\mathrm{div};\Omega)$-norm of the proposed finite element method for $\boldsymbol{H}(\mathrm{div};\Omega)$-elliptic interface problems. In Section 5, numerical experiments are presented to justify the theoretical prediction of the optimal convergence order. We summarize the work and point out future directions in Section 6.

2 Finite element approximation

We stick to the usual notations for Sobolev spaces $\boldsymbol{H}(\mathrm{div};\Omega)$, $\boldsymbol{H}_0(\mathrm{div};\Omega)$, etc, see [12, Chap. 1] or [21]. We also write

$$\boldsymbol{H}^1(\mathrm{div};\Omega) = \left\{ \mathbf{v} \in \boldsymbol{H}^1(\Omega) \mid \mathrm{div}\,\mathbf{v} \in H^1(\Omega) \right\} .$$

For a function u, we denote by u_i its restriction to Ω_i, i.e., $u_i := u|_{\Omega_i}$, for $i = 1, 2$.

2.1 Weak formulation

The weak formulation of (1.1)–(1.4) is straightforward and reads as follows:
Problem (Q) Seek $\mathbf{u} \in \boldsymbol{H}_0(\mathrm{div};\Omega)$ such that

$$a(\mathbf{u},\mathbf{v}) = \int_\Omega \mathbf{f}\cdot\mathbf{v}\,\mathrm{d}\mathbf{x} \qquad \forall\, \mathbf{v} \in \boldsymbol{H}_0(\mathrm{div};\Omega)\,, \tag{2.1}$$

with the bilinear form defined by

$$a(\mathbf{u},\mathbf{v}) := \sum_{i=1}^{2} \int_{\Omega_i} \left(\chi_i\,\mathrm{div}\,\mathbf{u}_i\cdot\mathrm{div}\,\mathbf{v}_i + \beta_i\mathbf{u}_i\cdot\mathbf{v}_i\right)\mathrm{d}\mathbf{x}\,. \tag{2.2}$$

By the assumptions on χ and β in Section 1, the bilinear forms $a(\cdot,\cdot)$ in (2.2) agrees with the $\boldsymbol{H}(\mathrm{div};\Omega)$-inner product of the Hilbert space $\boldsymbol{H}_0(\mathrm{div};\Omega)$ up to the weights χ_i's and β_i's, and the associated energy norm

$$\|\mathbf{u}\|_a = a(\mathbf{u},\mathbf{u})^{1/2} \tag{2.3}$$

is equivalent to the $\boldsymbol{H}(\mathrm{div};\Omega)$-norm. This ensures the existence and uniqueness of the solution of (2.1) by the Lax-Milgram Lemma [10, Theorem 1.1.3].

Throughout the paper, we assume that the solution of (2.1) has the regularity $\boldsymbol{H}_0(\mathrm{div};\Omega) \cap \boldsymbol{H}^1(\mathrm{div};\Omega_1) \cap \boldsymbol{H}^1(\mathrm{div};\Omega_2)$, which is a natural assumption in the present geometric setting.

2.2 Triangulations

Let the polyhedral domain $\Omega \in \mathbb{R}^3$ be equipped an oriented unstructured tetrahedral meshes $(\mathcal{T}_h)_h$ in the sense of [15, Def. 3], where h stands for the meshwidth. We denote by $\mathcal{F}_h$, $\mathcal{E}_h$ and $\mathcal{N}_h$ the respective sets of oriented faces, oriented edges and vertices of the triangulation $\mathcal{T}_h$. The quality of $\mathcal{T}_h$ can be gauged by means of its meshsize $h := \max_K h_K$, shape regularity measure $\rho(\mathcal{T}_h)$and quasi-uniformity measure $\gamma(\mathcal{T}_h)$ [8, Sect. 3] as follows

$$\rho(\mathcal{T}_h) := \max_{K\in\mathcal{T}_h} \frac{h_K}{r_K}, \quad h := \max_{K\in\mathcal{T}_h} h_K, \quad \gamma(\mathcal{T}_h) := \max_{K\in\mathcal{T}_h} \frac{h}{h_K},$$

where

$$\begin{aligned} h_K &:= \sup\{|\mathbf{x}-\mathbf{y}| : \mathbf{x},\mathbf{y}\in K\}, \\ r_K &:= \sup\{r>0 : \exists \mathbf{x}\in K;\, |\mathbf{x}-\mathbf{y}|<r \Rightarrow \mathbf{y}\in K\}. \end{aligned}$$

In the sequel, we will frequently denote by c and C generic positive constants which may depend on the domain Ω, the coefficients χ_i's, β_i's and the mesh parameters $\rho(\mathcal{T}_h)$ and $\gamma(\mathcal{T}_h)$, but must not depend on the meshwidth h and the related functions.

In the remainder of this section, we shall illustrate our assumptions on the triangulation in relation to the interface. First of all, our finite element discretization scheme relies heavily on the concept of *interface-aware triangulation*, see [16, Ass. 2.1]:

Assumption 2.1 (Interface-awareness)**.** *The triangulation $\mathcal{T}_h$ is* interface-aware *if for every $K \in \mathcal{T}_h$* all *its four vertices are either in $\overline{\Omega}_1$ or in $\overline{\Omega}_2$, and this element K is assumed to intersect with the interface Γ in such a way that at most three of its vertices are located on the interface Γ while all remaining vertices are either in Ω_1 or in Ω_2.*

Let us comment on Assumption 2.1 before we proceed. To meet the requirement of Assumption 2.1, the triangulation $\mathcal{T}_h$ should not be too coarse with respect to the interface, i.e., it is not allowed to have all the four vertices of an element $K \in \mathcal{T}_h$ located on the interface Γ. This might be the case for some element on a rather coarse triangulation surrounded by the interface of large curvature. Nevertheless, we can always refine the mesh until all the elements satisfies Assumption 2.1 owing to the smoothness of the interface.

When an element K satisfies $\overline{K} \cap \Gamma \neq \emptyset$, it is called an *interface element*, otherwise a *non-interface element*. The set of all interface elements is denoted by $\mathcal{T}_* := \{\, K \in \mathcal{T}_h \,|\, \overline{K} \cap \Gamma \neq \emptyset \,\}$ and $\mathcal{T}_*^i := \{\, K \in \mathcal{T}_* \,|\, \text{all nodes of } K \text{ are in } \overline{\Omega}_i \,\}$ represents the set of all interface elements of Ω_i, for $i = 1, 2$. For a fixed small $\delta > 0$, we define the *δ-strip regions* around the interface in Ω and Ω_i, $i = 1, 2$, respectively, by

$$S_\delta := \{\, x \in \Omega \,|\, \mathrm{dist}(x,\Gamma) < \delta \,\}, \quad S_\delta^i := \{\, x \in \Omega_i \,|\, \mathrm{dist}(x,\Gamma) < \delta \,\}, \quad i = 1, 2.$$

It is obvious that $S_\delta = S_\delta^1 \cup S_\delta^2 \cup \Gamma$ and $\mathcal{T}_* = \mathcal{T}_*^1 \cup \mathcal{T}_*^2$, and these δ-strip regions will be used for the error estimate near the interface, which in general cannot be captured using the techniques of standard interpolation approximation. For a vivid illustration of the concepts above, readers may refer to Figure 2 for a 2D scenario for better understanding.

According to Assumption 2.1, for any $K \in \mathcal{T}_*$, it must intersect with the interface Γ in one and only one of the following three situations

1. One vertex of K is located on the interface Γ, and the vertex located on the interface is called an *interface vertex*.
2. Two vertices of K are located on the interface Γ, and the oriented edge with two vertices on the interface is called an *interface edge*.

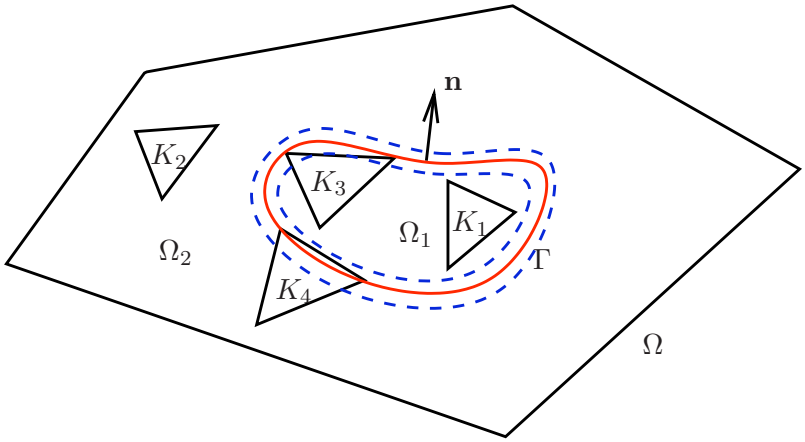

Figure 2: S_δ: the region of width 2δ between the two blue closed dashed lines around the interface Γ in red. Interface elements: $K_3 \in \mathcal{T}_*^1$, $K_4 \in \mathcal{T}_*^2$. Non-interface elements: $K_1 \in \mathcal{T}^1$, $K_2 \in \mathcal{T}^2$.

3. Three vertices of K are located on the interface Γ, and the triangular oriented face with three vertices on the interface is called an *interface face of the first kind*, while the face with only two vertices on the interface is called an *interface face of the second kind*.

And these notions are further illustrated by two typical interface elements intersecting the interface as shown in Figure 3.

For the sake of discretization, the smooth interface Γ has to be approximately resolved by tetrahedral meshes. We quantify the quality of the approximation of the smooth interface Γ by the triangulation $\mathcal{T}_h$ in terms of a parameter δ through the following definition, see [16, Def. 2.2]:

Definition 2.2. *The triangulation $\mathcal{T}_h$ is said to resolve the interface Γ* up to an error *δ if it can be decomposed as $\mathcal{T}_h = \mathcal{T}^1 \cup \mathcal{T}^2 \cup \mathcal{T}_*^1 \cup \mathcal{T}_*^2$, where*

$$\mathcal{T}^i = \{\, K \in \mathcal{T}_h \,;\quad K \subset \Omega_i \setminus S_\delta \,\}\,,$$

and $K \in \mathcal{T}_*^i$ if

$$\max\{\, \mathrm{dist}(x, \Gamma \cap K) \,;\quad x \in \overline{K} \cap \overline{\Omega}_{i'} \,\} \le \delta\,,$$

for $i = 1, 2$, where we define $i' = 1$ if $i = 2$ and $i' = 2$ if $i = 1$.

We may refer to Figure 2 for an illustration of Definition 2.2. It is worth remarking that although we assume that all vertices of an element K must belong to either subdomain Ω_1 or Ω_2, it is allowed that the interface may cut some elements into two parts lying in two different subdomains, see, for instance, triangle K_4 in Figure 2. By Definition 2.2 we easily see that any interface element K can be embedded in the union of the interface strip S_δ and one of the subdomains Ω_1 and Ω_2.

For a smooth interface Γ approximated by a union of triangular faces of the triangulation $\mathcal{T}_h$, we may further quantify the parameter δ in terms of the meshsize h as given by the next assumption.

Assumption 2.3. *The interface Γ is C^2-smooth. For the interface-aware meshes, there exists some δ of order h^2 for appropriately small h such that $K \cap \Omega_2 \subset S_\delta^2$ for all elements $K \in \mathcal{T}_*^1$, and $K \cap \Omega_1 \subset S_\delta^1$ for all elements $K \in \mathcal{T}_*^2$.*

A detailed proof of Assumption 2.3 of δ-approximation property for the interface-aware triangulation in two dimensions can be found in [9] using local coordinate system and the same idea can be easily extended to 3D with no essential changes.

For the subsequent error estimate, we will use a crucial perturbed interpolation operator. To that end, we first introduce three more helpful auxiliary concepts aided with the sketches in Figure 4.

Definition 2.4 (Interface twin edge)**.** *For any oriented interface edge $e_1 \in \mathcal{E}_h$, there exist two interface elements K_1 and K_2, with non-interface vertices $\mathbf{p}_1$ and $\mathbf{p}_2$, respectively, which share the interface edge e_1 and another interface vertex $\mathbf{q}_1$, such that there is a unique oriented curve $\widetilde{e}_1$*

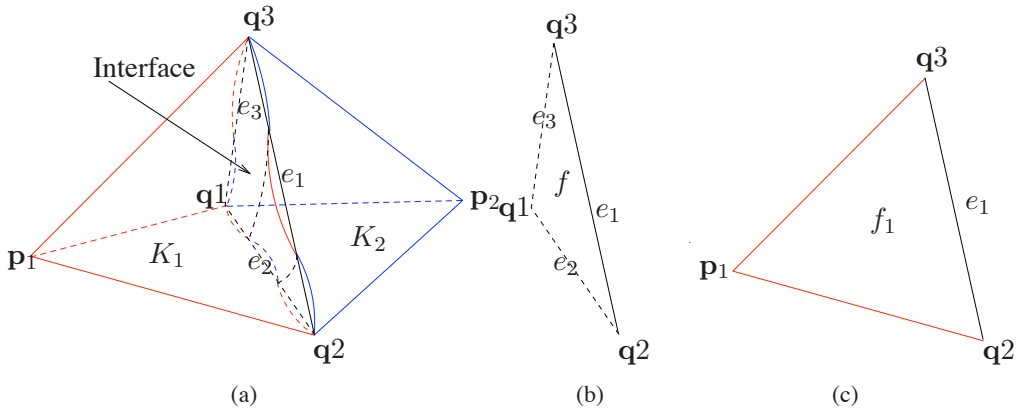

Figure 3: (a): Two typical tetrahedral interface elements K_1 and K_2 intersect with the interface Γ. The interface are visualized by the intersected piecewise smooth curves composed of blue and red curved segments on the surfaces of the tetrahedra K_1 and K_2. The interface edges are e_1, e_2 and e_3 denoted by black straight (dashed) line segments; (b): An interface face f of the first kind; (c): An interface face f_1 of the second kind.

which is the intersection of the interface and two triangular faces determined by $\mathbf{p}_1$ *with* e_1*, and* $\mathbf{p}_2$ *with* e_1*, respectively, and shares with* e_1 *the same starting and end points. We call* $\widetilde{e}_1$ *the* interface twin edge *associated with* e_1 *(see Figure 4(a) for an illustration).*

It is emphasized that any interface edge is always a straight line segment, and the associated interface twin edge could be a piecewise smooth curve (see, e.g., the alternating red and blue smooth curve $\widetilde{e}_1$ in Figure 4(a)) which shares the two endpoints with the interface edge e_1.

Definition 2.5 (Interface twin face of the first kind)**.** *For any oriented interface face of the first kind* $f \in \mathcal{F}_h$ *enclosed by three interface edges* $e_1, e_2, e_3 \in \mathcal{E}_h$*, with which three interface twin edges* $\widetilde{e}_1, \widetilde{e}_2, \widetilde{e}_3$ *are associated, respectively, there exists a unique smooth surface* $\widetilde{f}$ *on the interface circumscribed by* $\widetilde{e}_1, \widetilde{e}_2, \widetilde{e}_3$*. We call* $\widetilde{f}$ *an* interface twin face of the first kind *associated with the face* f*. The orientation of* $\widetilde{f}$ *is determined in the sense that it approximates that of* f *as meshes refine. (See Figure 4(b))*

Definition 2.6 (Interface twin face of the second kind)**.** *For any oriented interface face of the second kind* $f_1 \in \mathcal{F}_h$ *with an interface edge* $e_1 \in \mathcal{E}_h$*, with which the interface twin edge* $\widetilde{e}_1$ *are associated, if* f_1 *is an interface face of an interface element* $K \in \mathcal{T}_*^i$*,* $i = 1$ *or* 2*, then there exists a unique piecewise planar surface,*

$$\widetilde{f}_1 = (f_1 \cup S_{e_1,\widetilde{e}_1}) \setminus \overline{\Omega_{i'}}\,,$$

with $\setminus$ *being understood as set minus operation. The orientation of* $\widetilde{f}_1$ *is determined in such a way that* f_1 *and* $\widetilde{f}_1$ *share the same orientation as* f_1 *on* $f_1 \setminus S_{e_1,\widetilde{e}_1}$ *and* $\widetilde{f}_1$ *extends this orientation on the other part* $S_{e_1,\widetilde{e}_1} \setminus f_1$*. We call* $\widetilde{f}_1$ *an* interface twin face of the second kind *associated with the face* f_1*. (See Figure 4(c))*

For an oriented interface face of the second kind f_i consisting of one interface edge $e_i \in \mathcal{E}_h$ (with which the interface twin edges $\widetilde{e}_i$ are associated), we will need the following set

$$S_{e_i,\widetilde{e}_i} = (f_i \setminus \widetilde{f}_i) \cup (\widetilde{f}_i \setminus f_i)\,,$$

which denotes the slim open piecewise planar surface set surrounded by the curves e_i and $\widetilde{e}_i$, for $i = 1, 2, 3$. (See Figure 4(e))

For an interface face f of the first kind enclosed by three interface edges $e_1, e_2, e_3 \in \mathcal{E}_h$, with which three interface twin edges $\widetilde{e}_1, \widetilde{e}_2, \widetilde{e}_3$ are associated, respectively, we denote by $V_{f,\widetilde{f}}$ the closed volume set enclosed by the surfaces f, $\widetilde{f}$, $S_{e_1,\widetilde{e}_1}$, $S_{e_2,\widetilde{e}_2}$ and $S_{e_3,\widetilde{e}_3}$ (See Figure 4(d)). It is readily to

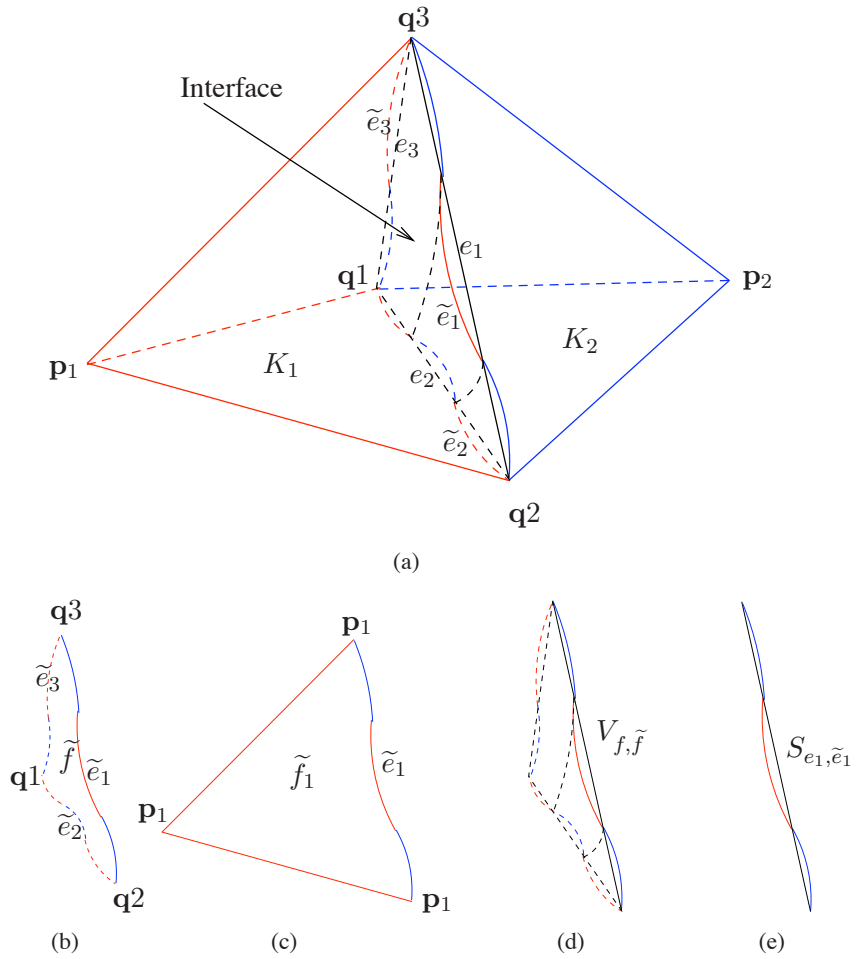

Figure 4: Illustration of interface twin edges and faces. (a): The interface twin edges are $\widetilde{e}_1$, $\widetilde{e}_2$ and $\widetilde{e}_3$ denoted by the piecewise smooth curves composed of blue and red curved segments on the interface; (b): An interface *twin* face $\widetilde{f}$ of the first kind; (c): An interface *twin* face $\widetilde{f}_1$ of the second kind; (d): small volume $V_{f,\widetilde{f}}$ sandwiched by interface (twin) faces of first kind; (e): slim area $S_{e_1,\widetilde{e}_1}$ enclosed by interface (twin) edges.

see by Assumption 2.3 that

$$V_{f,\widetilde{f}} \subset S_\delta \quad \text{and} \quad S_{e_i,\widetilde{e}_i} \subset S_\delta \quad \text{for } i = 1,2,3.$$

For the interface-aware triangulation, it is easy to deduce that

$$|V_{f,\widetilde{f}}| \sim \delta h^2, \qquad |S_{e_i,\widetilde{e}_i}| \sim \delta h \tag{2.4}$$

where $|\cdot|$ represents either volume or area measures.

In the sequel, the triangulation $\mathcal{T}_h$ will be assumed to be sufficiently fine to allow the existence of interface twin edges. For some interface with bizarre geometry the interface twin edges might not be well defined for certain coarse meshes. But due to the C^2-smoothness of the interface, we can always refine the mesh till a desired interface twin edge (resp. the associated interface twin face) is obtained for any interface edge.

2.3 Finite element discretization

A suitable trial space $\mathbf{F}_h \subset \boldsymbol{H}_0(\mathrm{div};\Omega)$ for the Galerkin discretization of (2.1) is supplied by the lowest order Raviart-Thomas elements of the first family (see, e.g., [5,22]), that is,

$$\mathbf{F}_h := \left\{ \mathbf{v}_h \in \boldsymbol{H}_0(\mathrm{div};\Omega) \mid \mathbf{v}_h|_K(\mathbf{x}) = \mathbf{a}_K + b_K\mathbf{x},\, \mathbf{a}_K \in \mathbb{R}^3,\, b_K \in \mathbb{R},\, \mathbf{x} \in K,\, \forall K \in \mathcal{T}_h \right\} .$$

Writing $\widehat{\mathcal{F}}_h$ for the set of all interior faces of $\mathcal{T}_h$, the degrees of freedom of $\mathbf{F}_h$ are given by the surface integrals

$$\mathbf{v}_h \mapsto \int_f \mathbf{v}_h \cdot \mathbf{n}\, \mathrm{d}S\,, \quad f \in \widehat{\mathcal{F}}_h\,.$$

It is well established that there exists a well-defined global finite element interpolation operator $\boldsymbol{\Pi}_h : \boldsymbol{H}^1(\mathrm{div};\Omega) \mapsto \mathbf{F}_h$ (cf. [21, Thm. 5.25, Sect. 5.4]), which has the following approximation property.

Lemma 2.7. *The interpolation operator $\boldsymbol{\Pi}_h$ possesses the optimal approximation property*

$$\exists C = C(\rho(\mathcal{T}_h)) : \quad \|\mathbf{u} - \boldsymbol{\Pi}_h\mathbf{u}\|_{\boldsymbol{H}(\mathrm{div};\Omega)} \le Ch\|\mathbf{u}\|_{\boldsymbol{H}^1(\mathrm{div};\Omega)}\ \forall\, \mathbf{u} \in \boldsymbol{H}^1(\mathrm{div};\Omega)\,. \tag{2.5}$$

Moreover, we recall that face elements are an affine equivalent family of finite elements with respect to the pullback transformation (see [15,21])

$$\mathsf{B}\widehat{\mathbf{v}}(\widehat{\mathbf{x}}) := \det(\mathsf{B})\mathbf{v}(\mathbf{x})\,, \quad \mathbf{x} = \mathsf{B}\widehat{\mathbf{x}} + \mathbf{t}\,, \quad \mathsf{B} \in \mathbb{R}^{3,3},\, \mathbf{t} \in \mathbb{R}^3\,. \tag{2.6}$$

On a tetrahedron K with vertices $[\mathbf{a}_1,\mathbf{a}_2,\mathbf{a}_3,\mathbf{a}_4]$ and barycentric coordinates $\lambda_1,\lambda_2,\lambda_3,\lambda_4$, the local shape function associated with a face $f = [\mathbf{a}_i,\mathbf{a}_j,\mathbf{a}_k]$ are given by (see [15, Sect. 3.2])

$$\begin{aligned}\mathbf{b}_K^f = 2(&\lambda_i\, \mathbf{grad}\,\lambda_j \times \mathbf{grad}\,\lambda_k + \lambda_j\, \mathbf{grad}\,\lambda_k \times \mathbf{grad}\,\lambda_i \\ &+\lambda_k\, \mathbf{grad}\,\lambda_i \times \mathbf{grad}\,\lambda_j)\,, \quad 1 \le i < j < k \le 4\,.\end{aligned} \tag{2.7}$$

They can be assembled into a collection of global bases $\{\mathbf{b}_i,\, i = 1,\ldots,\sharp\widehat{\mathcal{F}}_h\}$ of $\mathbf{F}_h$.

The following lemma can be shown by adapting the proof of [15, Lemma 3.12] to bound the local basis functions in terms of the mesh size h.

Lemma 2.8. *Let $\mathcal{T}_h$ be a quasi-uniform, oriented unstructured tetrahedral mesh in Ω with meshsize h. Then there exist some positive constants C such that the local basis functions $\mathbf{b}_K^f$, $f \subset \partial K$, satisfy the following error estimates*

$$\|\mathbf{b}_K^f\|^2_{\boldsymbol{H}(\mathrm{div};K)} \le \frac{C}{h}\,, \qquad \|\operatorname{div}\mathbf{b}_K^f\|^2_{\boldsymbol{H}(\mathrm{div};K)} \le \frac{C}{h^3}\,. \tag{2.8}$$

With the finite element function spaces presented above, the finite element approximation of (2.1) can be stated as follows:

Problem ($\mathbf{Q}_h$) Seek $\mathbf{u}_h \in \mathbf{F}_h$ such that

$$a(\mathbf{u}_h, \mathbf{v}_h) = \int_\Omega \mathbf{f} \cdot \mathbf{v}_h \, \mathrm{d}\mathbf{x} \qquad \forall\, \mathbf{v}_h \in \mathbf{F}_h \,. \tag{2.9}$$

The existence and uniqueness of the solution of (2.9) follow from the Lax-Milgram Lemma [10, Theorem 1.1.3], similar to those of the continuous problem ($\mathbf{Q}$). One natural idea to derive the estimate of discretization error is through the best approximation error estimate in light of the quasi-optimality from Cea's lemma. But this is only possible, if the Galerkin matrix is computed exactly.

The exact evaluation of the stiffness matrix associated with the bilinear form $a(\cdot,\cdot)$ in (2.9) can be very complicated on an interface element when it is cut through by the interface, especially in three dimensions. A much more convenient formulation is obtained by replacing the original bilinear form (2.2) with an approximate bilinear form $a_h(\cdot,\cdot)$:

$$a_h(\mathbf{u}_h, \mathbf{v}_h) = \sum_{K\in\mathcal{T}} \int_K \left(\chi_K \operatorname{div} \mathbf{u}_h \cdot \operatorname{div} \mathbf{v}_h + \beta_K \mathbf{u}_h \cdot \mathbf{v}_h\right) \mathrm{d}\mathbf{x}\,, \tag{2.10}$$

where the coefficients χ_K's and β_K's are elementwise constant. In our present setting of piecewise constant coefficients, for every $K \in \mathcal{T}$, $\chi_K = \chi_i$ ($\beta_K = \beta_i$, resp.) if $K \in \mathcal{T}^i$ or $\mathcal{T}^i_*$ for $i \in \{1, 2\}$.

With the modified bilinear form in (2.10), we can now define a more practical finite element method for the variational problem ($\mathbf{Q}$) by replacing $a(\cdot,\cdot)$ by $a_h(\cdot,\cdot)$.

Problem ($\widetilde{\mathbf{Q}}_h$) Find $\mathbf{u}_h \in \mathbf{F}_h$ such that

$$a_h(\mathbf{u}_h, \mathbf{v}_h) = \int_\Omega \mathbf{f} \cdot \mathbf{v}_h \, \mathrm{d}\mathbf{x} \qquad \forall\, \mathbf{v}_h \in \mathbf{F}_h. \tag{2.11}$$

It can be immediately seen that the bilinear form $a_h(\cdot,\cdot)$ still preserves coercivity and continuity, and thus the well-posedness of Problem ($\widetilde{\mathbf{Q}}_h$) is assured. Moreover, the two bilinear forms a_h and a are related to each other by

$$a(\mathbf{u}, \mathbf{v}) = a_h(\mathbf{u}, \mathbf{v}) + a^\Delta(\mathbf{u}, \mathbf{v}), \tag{2.12}$$

where the residual bilinear form $a^\Delta(\cdot,\cdot)$ satisfies

$$|a^\Delta(\mathbf{u}, \mathbf{v})| \le C \|\mathbf{u}\|_{\boldsymbol{H}(\operatorname{div};S_\delta)} \|\mathbf{v}\|_{\boldsymbol{H}(\operatorname{div};S_\delta)}, \tag{2.13}$$

with the constant C depending only on the coefficients χ_i's and β_i's.

2.4 Interface-aware interpolation operator

The modification of the bilinear form for ease of computation of stiffness matrix complicates the error estimate quite a lot. We have to recover quasi-optimality by taking into account numerical crime. It is worth remarking that there are no ambiguities of the interpolation operator $\boldsymbol{\Pi}_h$ when applied for functions in $\boldsymbol{H}_0(\operatorname{div};\Omega) \cap \boldsymbol{H}^1(\operatorname{div};\Omega_1) \cap \boldsymbol{H}^1(\operatorname{div};\Omega_2)$, but the corresponding interpolant is not a good candidate to yield best approximation error estimate. It is worth pointing out that the original idea to derive error estimate by combining Cea's lemma with interpolation error estimate of $\boldsymbol{\Pi}_h$, which works in $\boldsymbol{H}(\operatorname{div};\Omega)$-elliptic problems, fails in $\boldsymbol{H}(\operatorname{div};\Omega)$-elliptic interface one. Instead we shall define a problem-specific interface-aware interpolation operator, which can be viewed as a perturbed version of $\boldsymbol{\Pi}_h$. The pivotal idea is to define a perturbed degree of freedom for each interface face of an interface element by a surrogate degree of freedom defined through the interface twin face. To be more precise, we elucidate the idea in the following definition, *cf.* [16, Sect. 2.4].

Definition 2.9 (Interface-aware interpolation operators)**.** *Let $\mathcal{T}_h$ be an oriented unstructured tetrahedral triangulation satisfying Assumptions 2.1 and 2.3 with mesh size h, and $\mathbf{F}_h$ the lowest order Raviart-Thomas elements on $\mathcal{T}_h$.*

For a function $\mathbf{u} \in \boldsymbol{H}_0(\operatorname{div};\Omega) \cap \boldsymbol{H}^1(\operatorname{div};\Omega_1) \cap \boldsymbol{H}^1(\operatorname{div};\Omega_2)$, we define a perturbed *interface-aware interpolation operator*

$$\widetilde{\boldsymbol{\Pi}}_h : \boldsymbol{H}_0(\operatorname{div};\Omega) \cap \boldsymbol{H}^1(\operatorname{div};\Omega_1) \cap \boldsymbol{H}^1(\operatorname{div};\Omega_2) \mapsto \mathbf{F}_h$$

and its interpolation $\widetilde{\mathbf{\Pi}}_h$ as follows:

$$\int_f \widetilde{\mathbf{\Pi}}_h \mathbf{u} \cdot \mathbf{n}\, \mathrm{d}S = \begin{cases} \int_f \mathbf{u} \cdot \mathbf{n}\, \mathrm{d}S, & \text{if } f \in \mathcal{F}_h \text{ is a non-interface face;} \\ \int_{\widetilde{f}} \mathbf{u} \cdot \mathbf{n}\, \mathrm{d}S, & \text{if } f \in \mathcal{F}_h \text{ is an interface face associated} \\ & \quad \text{with an interface twin face } \widetilde{f}. \end{cases}$$

We remark that the interface-aware interpolation operator $\widetilde{\mathbf{\Pi}}_h$ is introduced only for the subsequent theoretical error estimates, and it is not needed in the numerical implementation of the finite element method $(\widetilde{\mathbf{Q}}_h)$.

3 Theoretical tools

In this section, we supply some technical results which are indispensable tools for the subsequent convergence analysis of finite element methods for $\boldsymbol{H}(\mathrm{div};\Omega)$-elliptic interface problems.

We first recall an important inequality, under the same problem setting as in Section 1, which will be used for the error estimate in the region near the smooth interface. The proof is similar to that of [19, Lemma 2.1].

Lemma 3.1. *Let $i \in \{1,2\}$. Then it holds for any $z_i \in H^1(\Omega_i)$ that*

$$\|z_i\|_{L^2(S_\delta^i)} \le C\sqrt{\delta}\|z_i\|_{H^1(\Omega_i)},$$

provided that δ is sufficiently small. Here the constant C depends only on the smooth interface and the domain Ω.

There is a straightforward corollary to Lemma 3.1 which can be viewed as its vectorized version in $\boldsymbol{H}^1(\mathrm{div})$ spaces by simply using the Cauchy-Schwarz inequality.

Corollary 3.2 (δ-strip argument)**.** *Let $i \in \{1,2\}$. Then it holds for any $z_i \in \boldsymbol{H}^1(\mathrm{div};\Omega_i)$ that*

$$\|z_i\|_{\boldsymbol{H}(\mathrm{div};S_\delta^i)} \le C\sqrt{\delta}\|z_i\|_{\boldsymbol{H}^1(\mathrm{div};\Omega_i)}$$

provided that δ is sufficiently small. The constant C depends only on the smooth interface and the domain Ω.

Next, motivated by the construction of extension operators for functions in Sobolev spaces $H^k(\Omega)$ [1,11], we develop in this subsection a new extension theorem for functions in the $\boldsymbol{H}^1(\mathrm{div})$ space. This new extension result will play a crucial role in the subsequent error estimate on interface elements.

It is well-known that (see, e.g., [11, Theorem 1, Sec. 5.4]) for a connected bounded domain in $U \subset \mathbb{R}^3$ with C^2-smooth boundary there exists a bounded linear extension operator

$$E : H^2(U) \to H^2(\mathbb{R}^3)$$

such that for any scalar function $u \in H^2(U)$:

1. $Eu = u$ a.e. in U.
2. $\|Eu\|_{H^2(\mathbb{R}^3)} \le C\|u\|_{H^2(U)}$ with the constant C depending only on U.

Compared with the extension of scalar functions, vector fields must be extended in a more delicate way to conserve their properties. In [16, Thm. 4.3], the following $\boldsymbol{H}^1(\mathbf{curl})$-extension theorem is proved based on the commuting diagram property [15]:

$$\mathbf{E}_{\mathbf{curl}}(\mathbf{grad}\, p) = \mathbf{grad}(Ep). \tag{3.1}$$

Theorem 3.3 ($\boldsymbol{H}^1(\mathbf{curl})$-extension theorem)**.** *Assuming that U is a connected bounded domain in $\mathbb{R}^3$ with C^2-smooth boundary. Then there exists a bounded linear extension operator:*

$$\mathbf{E}_{\mathbf{curl}} \ : \ \boldsymbol{H}^1(\mathbf{curl};U) \to \boldsymbol{H}^1(\mathbf{curl};\mathbb{R}^3), \tag{3.2}$$

such that for each $\mathbf{u} \in \boldsymbol{H}^1(\mathbf{curl};U)$:

1. $\mathbf{E}_{\mathbf{curl}}\mathbf{u} = \mathbf{u}$ *a.e. in* U.

2. $\|\mathbf{E}_{\mathbf{curl}}\mathbf{u}\|_{\boldsymbol{H}^1(\mathbf{curl};\mathbb{R}^3)} \leq C\,\|\mathbf{u}\|_{\boldsymbol{H}^1(\mathbf{curl};U)}$, *with the constant* C *depending only on* U.

Analogously, suppose $\mathbf{u} \in \boldsymbol{H}^1(\mathrm{div};U)$ and we wish to extend $\mathbf{u}$ to be a function $\widetilde{\mathbf{u}} \in \boldsymbol{H}^1(\mathrm{div};\mathbb{R}^3)$. Since for a vector-valued function $\mathbf{w} \in \boldsymbol{H}^1(\mathbf{curl};U)$ we have $\mathbf{curl}\,\mathbf{w} \in \boldsymbol{H}^1(\mathrm{div};U)$, it seems promising to define an $\boldsymbol{H}^1(\mathrm{div})$-extension operator $\mathbf{E}_{\mathrm{div}}$ still based on the commuting diagram property [15]:

$$\mathbf{E}_{\mathrm{div}}(\mathbf{curl}\,\mathbf{w}) = \mathbf{curl}(\mathbf{E}_{\mathbf{curl}}\mathbf{w}). \tag{3.3}$$

With such motivation, we are now able to show the $\boldsymbol{H}^1(\mathrm{div})$-extension theorem across the smooth boundary, whose proof will be given in detail in Appendix A.

Theorem 3.4 ($\boldsymbol{H}^1(\mathrm{div})$-extension theorem)**.** *Assume that* U *is a connected bounded domain in* $\mathbb{R}^3$ *with* C^2*-smooth boundary. Then there exists a bounded linear extension operator:*

$$\mathbf{E}_{\mathrm{div}} \;:\; \boldsymbol{H}^1(\mathrm{div};U) \to \boldsymbol{H}^1(\mathrm{div};\mathbb{R}^3) \quad i = 1,2, \tag{3.4}$$

such that for each $\mathbf{u} \in \boldsymbol{H}^1(\mathrm{div};U)$*:*

1. $\mathbf{E}_{\mathrm{div}}\mathbf{u} = \mathbf{u}$ *a.e. in* U.

2. $\|\mathbf{E}_{\mathrm{div}}\mathbf{u}\|_{\boldsymbol{H}^1(\mathrm{div};\mathbb{R}^3)} \leq C\,\|\mathbf{u}\|_{\boldsymbol{H}^1(\mathrm{div};U)}$, *with the constant* C *depending only on* U.

For our subsequent analysis, we need the following special version of Theorem 3.4.

Corollary 3.5. *There exist two bounded linear operators*

$$\mathbf{E}^i_{\mathrm{div}} \;:\; \boldsymbol{H}^1(\mathrm{div};\Omega_i) \to \boldsymbol{H}^1(\mathrm{div};\Omega) \quad i = 1,2, \tag{3.5}$$

such that for each $\mathbf{u} \in \boldsymbol{H}^1(\mathrm{div};\Omega_i)$*:*

1. $\mathbf{E}^i_{\mathrm{div}}\mathbf{u} = \mathbf{u}$ *a.e. in* Ω_i.

2. $\left\|\mathbf{E}^i_{\mathrm{div}}\mathbf{u}\right\|_{\boldsymbol{H}^1(\mathrm{div};\Omega)} \lesssim \|\mathbf{u}\|_{\boldsymbol{H}^1(\mathrm{div};\Omega_i)}$.

Proof. Noticing Assumption 2.3 that the interface Γ is C^2-smooth, and some slight modification of the proof of Theorem 3.4 yields the desired result. □

The following inequality in a pyramid can be found in [16, Lemma 3.6], and will be applied to the error estimates in those pyramids with slender bottom faces in the next section.

Lemma 3.6. *Let* P *be a pyramid with* F *being its quadrilateral bottom face and* O *its apex (see Figure 5). Then we have*

$$\|u\|^2_{L^2(F)} \leq \frac{3}{d}\|u\|_{L^2(P)}(h_P\|\mathbf{grad}\,u\|_{L^2(P)} + \|u\|_{L^2(P)}) \quad \forall u \in H^1(P)\,,$$

where $d := \mathrm{dist}(O,F)$, $h_P := \max\{|\mathbf{x}-\mathbf{y}| : \mathbf{x},\mathbf{y} \in P\}$*. Moreover, if* $d \sim O(h_P)$ *and* $h_P < 1$*, we have*

$$\|u\|^2_{L^2(F)} \leq C\left(\frac{1}{h_P}\|u\|^2_{L^2(P)} + \|\mathbf{grad}\,u\|^2_{L^2(P)}\right) \quad \forall u \in H^1(P)\,, \tag{3.6}$$

with $C > 0$ *independent of* h_P.

4 Convergence analysis

In this section, we show the optimal convergence for the $\boldsymbol{H}(\mathrm{div})$-elliptic interface problem using the lowest order $\boldsymbol{H}(\mathrm{div};\Omega)$-conforming finite element approximation. We first state a technical lemma to be used for the convergence theorem.

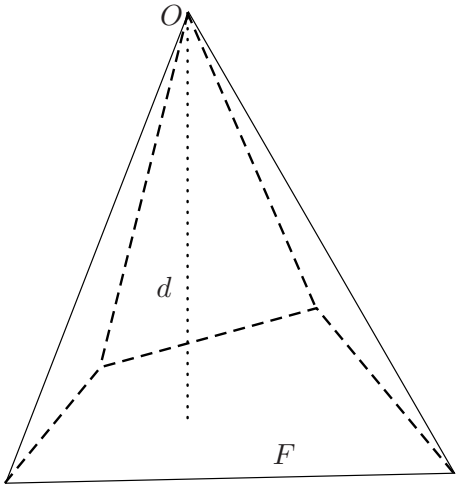

Figure 5: Sketch of the pyramid in Lemma 3.6.

Lemma 4.1. *Let* $\mathbf{u} \in \boldsymbol{H}_0(\mathrm{div};\Omega) \cap \boldsymbol{H}^1(\mathrm{div};\Omega_1) \cap \boldsymbol{H}^1(\mathrm{div};\Omega_2)$. *Then we have*

$$\sum_{K\in\mathcal{T}_*^1} \|\mathbf{E}^1_{\mathrm{div}}\mathbf{u}_1\|^2_{\boldsymbol{H}(\mathrm{div};K\cap\Omega_2)} \leq \|\mathbf{E}^1_{\mathrm{div}}\mathbf{u}_1\|^2_{\boldsymbol{H}(\mathrm{div};S^2_\delta)} \leq C\delta\|\mathbf{u}_1\|^2_{\boldsymbol{H}^1(\mathrm{div};\Omega_1)}, \tag{4.1}$$

$$\sum_{K\in\mathcal{T}_*^1} \|\mathbf{u}_2\|^2_{\boldsymbol{H}(\mathrm{div};K\cap\Omega_2)} \leq \|\mathbf{u}_2\|^2_{\boldsymbol{H}(\mathrm{div};S^2_\delta)} \leq C\delta\|\mathbf{u}_2\|^2_{\boldsymbol{H}^1(\mathrm{div};\Omega_2)}\,. \tag{4.2}$$

Analogously,

$$\sum_{K\in\mathcal{T}_*^2} \|\mathbf{E}^2_{\mathrm{div}}\mathbf{u}_2\|^2_{\boldsymbol{H}(\mathrm{div};K\cap\Omega_1)} \leq \|\mathbf{E}^2_{\mathrm{div}}\mathbf{u}_2\|^2_{\boldsymbol{H}(\mathrm{div};S^1_\delta)} \leq C\delta\|\mathbf{u}_2\|^2_{\boldsymbol{H}^1(\mathrm{div};\Omega_2)}, \tag{4.3}$$

$$\sum_{K\in\mathcal{T}_*^2} \|\mathbf{u}_1\|^2_{\boldsymbol{H}(\mathrm{div};K\cap\Omega_1)} \leq \|\mathbf{u}_1\|^2_{\boldsymbol{H}(\mathrm{div};S^1_\delta)} \leq C\delta\|\mathbf{u}_1\|^2_{\boldsymbol{H}^1(\mathrm{div};\Omega_1)}\,. \tag{4.4}$$

Proof. We only prove (4.1)–(4.2) since the estimates (4.3)–(4.4) can be shown in exactly the same manner. To see (4.1), we note $\cup_{K\in\mathcal{T}_*^1} K\cap\Omega_2 \subset S^2_\delta$ and that all elements of $\mathcal{T}_h$ are pairwise disjoint, the first inequality in (4.1) follows immediately from Assumption 2.3. For the second estimate, using the Corollary 3.2 and the continuity property of the extension operator $\mathbf{E}^1_{\mathrm{div}}$ yields

$$\|\mathbf{E}^1_{\mathrm{div}}\mathbf{u}_1\|^2_{\boldsymbol{H}(\mathrm{div};S^2_\delta)} \leq C\delta\|\mathbf{E}^1_{\mathrm{div}}\mathbf{u}_1\|^2_{\boldsymbol{H}^1(\mathrm{div};\Omega_2)} \leq C\delta\|\mathbf{u}_1\|^2_{\boldsymbol{H}^1(\mathrm{div};\Omega_1)}\,.$$

The estimate (4.2) is obtained analogously by noting the fact that $\cup_{K\in\mathcal{T}_*^1} K\cap\Omega_2 \subset S^2_\delta$. ☐

To obtain the convergence result, we need to show an appropriate interpolation error estimate for the interface-aware interpolation operator $\widetilde{\boldsymbol{\Pi}}_h$ in Definition. 2.9. The following estimate is the counterpart of [16, Lemma 4.2], with a much more involved proof, however, due to more complicated geometrical considerations.

Lemma 4.2. *Let* $\mathbf{u} \in \boldsymbol{H}_0(\mathrm{div};\Omega) \cap \boldsymbol{H}^1(\mathrm{div};\Omega_1) \cap \boldsymbol{H}^1(\mathrm{div};\Omega_2)$. *Then we have*

$$\left\|\mathbf{u} - \widetilde{\boldsymbol{\Pi}}_h\mathbf{u}\right\|_{\boldsymbol{H}(\mathrm{div};\Omega)} \quad\leq\quad C(h + \sqrt{\delta} + \frac{\delta}{\sqrt{h}})\left(\|\mathbf{u}\|_{\boldsymbol{H}^1(\mathrm{div};\Omega_1)} + \|\mathbf{u}\|_{\boldsymbol{H}^1(\mathrm{div};\Omega_2)}\right) \tag{4.5}$$

with constant $C > 0$ *depending on* $\rho(\mathcal{T}_h)$, $\gamma(\mathcal{T}_h)$ *and* Ω, *but independent of* h, δ *and* $\mathbf{u}$.

Proof. Let $K \in \mathcal{T}_*^1$. We notice the crucial identity is

$$\widetilde{\boldsymbol{\Pi}}_h\mathbf{u}\Big|_K = \widetilde{\boldsymbol{\Pi}}_h\mathbf{E}^1_{\mathrm{div}}\mathbf{u}\Big|_K\,.$$

Then we can decompose the difference $\mathbf{u}-\widetilde{\mathbf{\Pi}}_h\mathbf{u}$ over K into three parts:

$$\begin{aligned}\left(\mathbf{u}-\widetilde{\mathbf{\Pi}}_h\mathbf{u}\right)\Big|_K =\ & \left(\mathbf{u}-\mathbf{E}^1_{\mathrm{div}}\mathbf{u}\right)\big|_K+\left(\mathbf{E}^1_{\mathrm{div}}\mathbf{u}-\mathbf{\Pi}_h\mathbf{E}^1_{\mathrm{div}}\mathbf{u}\right)\big|_K\\ &+\left(\mathbf{\Pi}_h\mathbf{E}^1_{\mathrm{div}}\mathbf{u}-\widetilde{\mathbf{\Pi}}_h\mathbf{E}^1_{\mathrm{div}}\mathbf{u}\right)\Big|_K .\end{aligned} \tag{4.6}$$

Noting that $\mathbf{u}=\mathbf{E}^1_{\mathrm{div}}\mathbf{u}$ on $K\cap\Omega_1$ and employing Lemma 4.1 leads to

$$\begin{aligned}&\sum_{K\in\mathcal{T}^1_*}\left\|\mathbf{u}-\mathbf{E}^1_{\mathrm{div}}\mathbf{u}\right\|^2_{\boldsymbol{H}(\mathrm{div};K)}=\sum_{K\in\mathcal{T}^1_*}\left\|\mathbf{u}-\mathbf{E}^1_{\mathrm{div}}\mathbf{u}\right\|^2_{\boldsymbol{H}(\mathrm{div};K\cap\Omega_2)}\\ &\le C\sum_{K\in\mathcal{T}^1_*}\|\mathbf{u}\|^2_{\boldsymbol{H}(\mathrm{div};K\cap\Omega_2)}+\sum_{K\in\mathcal{T}^1_*}\left\|\mathbf{E}^1_{\mathrm{div}}\mathbf{u}\right\|^2_{\boldsymbol{H}(\mathrm{div};K\cap\Omega_2)}\\ &\le C\delta\|\mathbf{u}\|^2_{\boldsymbol{H}^1(\mathrm{div};\Omega_1)} .\end{aligned} \tag{4.7}$$

A classical interpolation result ([21, Theorem 5.25, pp. 124]) for the standard interpolation operator $\mathbf{\Pi}_h$ and the continuous property of $\mathbf{E}^1_{\mathrm{div}}$ give

$$\begin{aligned}&\sum_{K\in\mathcal{T}^1_*}\left\|\mathbf{E}^1_{\mathrm{div}}\mathbf{u}-\mathbf{\Pi}_h\mathbf{E}^1_{\mathrm{div}}\mathbf{u}\right\|^2_{\boldsymbol{H}(\mathrm{div};K)}\le C\sum_{K\in\mathcal{T}^1_*}h^2\left\|\mathbf{E}^1_{\mathrm{div}}\mathbf{u}\right\|^2_{\boldsymbol{H}^1(\mathrm{div};K)}\\ &\le Ch^2\left\|\mathbf{E}^1_{\mathrm{div}}\mathbf{u}\right\|^2_{\boldsymbol{H}^1(\mathrm{div};\Omega)}\le Ch^2\|\mathbf{u}\|^2_{\boldsymbol{H}^1(\mathrm{div};\Omega_1)} .\end{aligned} \tag{4.8}$$

The most challenging issue comes from the third term in the right hand side of (4.6), where we observe that the only difference between two interpolation functions involved lies in the degrees of freedom associated with the interface faces of first and second kind. Without loss of generality, let us consider a typical case, namely picking up the interface element K_1 as shown in Figure 4(a) as our current K and assuming that most part of K_1 lies in Ω_1.

We shall investigate the error estimate in K_1 in detail step by step with reference to Figure 4. First of all, we have by the definition of $\mathbf{\Pi}_h$ and $\widetilde{\mathbf{\Pi}}_h$

$$\begin{aligned}&\left\|\mathbf{\Pi}_h\mathbf{E}^1_{\mathrm{div}}\mathbf{u}-\widetilde{\mathbf{\Pi}}_h\mathbf{E}^1_{\mathrm{div}}\mathbf{u}\right\|^2_{\boldsymbol{H}(\mathrm{div};K_1)}\\ &=\left\|\left(\int_f\mathbf{E}^1_{\mathrm{div}}\mathbf{u}\cdot\mathrm{d}\vec{S}-\int_{\widetilde{f}}\mathbf{E}^1_{\mathrm{div}}\mathbf{u}\cdot\mathrm{d}\vec{S}\right)\mathbf{b}_f+\sum_{i=1}^3\left(\int_{f_i}\mathbf{E}^1_{\mathrm{div}}\mathbf{u}\cdot\mathrm{d}\vec{S}-\int_{\widetilde{f}_i}\mathbf{E}^1_{\mathrm{div}}\mathbf{u}\cdot\mathrm{d}\vec{S}\right)\mathbf{b}_{f_i}\right\|^2_{\boldsymbol{H}(\mathrm{div};K_1)}\end{aligned}$$

Without loss of generality, all basis functions $\mathbf{b}_{f_i}, i=1,2,3$ and $\mathbf{b}_f$ refer to outgoing fluxes with normal vectors pointing outward. Here we play the trick to enclose $V_{f,\widetilde{f}}$ by adding $S_{e_i,\widetilde{e}_i}, i=1,2,3$ to f and $-\widetilde{f}$ (which means $\widetilde{f}$ with opposite orientation) and subtracting the surplus. Note that for h sufficiently small, the orientations of f and $\widetilde{f}$ are approximately the same as indicated by the outward normal direction $\mathbf{n}$ in Figure 6(a) and (b). Note that the orientations of $S_{e_i,\widetilde{e}_i}$'s depends only on those of f_i and $\widetilde{f}_i$.

Then the equality above can be rewritten as the following crucial identity:

$$\begin{aligned}&\left\|\left(\int_f\mathbf{E}^1_{\mathrm{div}}\mathbf{u}\cdot\mathrm{d}\vec{S}-\int_{\widetilde{f}}\mathbf{E}^1_{\mathrm{div}}\mathbf{u}\cdot\mathrm{d}\vec{S}\right)\mathbf{b}_f+\sum_{i=1}^3\left(\int_{f_i}\mathbf{E}^1_{\mathrm{div}}\mathbf{u}\cdot\mathrm{d}\vec{S}-\int_{\widetilde{f}_i}\mathbf{E}^1_{\mathrm{div}}\mathbf{u}\cdot\mathrm{d}\vec{S}\right)\mathbf{b}_{f_i}\right\|^2_{\boldsymbol{H}(\mathrm{div};K_1)}\\ &=\left\|\left(\int_{f\cup(-\widetilde{f})\cup S_{e_1,\widetilde{e}_1}\cup S_{e_2,\widetilde{e}_2}\cup S_{e_3,\widetilde{e}_3}}\mathbf{E}^1_{\mathrm{div}}\mathbf{u}\cdot\mathrm{d}\vec{S}\right)\mathbf{b}_f+\sum_{i=1}^3\left(\int_{S_{e_i,\widetilde{e}_i}}\mathbf{E}^1_{\mathrm{div}}\mathbf{u}\cdot\mathrm{d}\vec{S}\right)(\mathbf{b}_{f_i}-\mathbf{b}_f)\right\|^2_{\boldsymbol{H}(\mathrm{div};K_1)}\\ &:=\|\Theta+\Lambda\|^2_{\boldsymbol{H}(\mathrm{div};K_1)}\end{aligned}$$

An insightful observation of the orientations of $f,\widetilde{f},S_{e_1,\widetilde{e}_1},S_{e_2,\widetilde{e}_2}$ and $S_{e_3,\widetilde{e}_3}$ enables us to apply

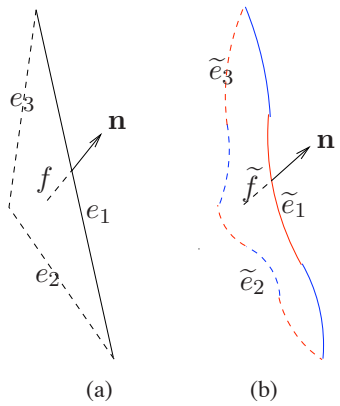

Figure 6: Orientations of interface (twin) faces.

the divergence law to further estimate Θ.

$$\|\Theta\|^2_{\boldsymbol{H}(\mathrm{div};K_1)} \le C\,\|\mathbf{b}_f\|^2_{\boldsymbol{H}(\mathrm{div};K_1)} \left(\int_{V_{f,\tilde{f}}} \mathrm{div}\,\mathbf{E}^1_{\mathrm{div}}\mathbf{u}\,\mathrm{d}V\right)^2$$
$$\le C\frac{1}{h^3}\left(\int_{V_{f,\tilde{f}}} \mathrm{div}\,\mathbf{E}^1_{\mathrm{div}}\mathbf{u}\,\mathrm{d}V\right)^2 \le C\frac{|V_{f,\tilde{f}}|}{h^3}\left(\int_{V_{f,\tilde{f}}} |\,\mathrm{div}\,\mathbf{E}^1_{\mathrm{div}}\mathbf{u}|^2\,\mathrm{d}V\right),$$

where we employ the $H(\mathrm{div})$-estimates for the basis function $\mathbf{b}_f$ in Lemma 2.8 in the second inequality and use the Cauchy-Schwarz inequality in the third one.

Another important observation is the following divergence-free property:

$$\mathrm{div}(\mathbf{b}_K^{f_1} - \mathbf{b}_K^{f_2}) = 0, \tag{4.9}$$

where f_1, f_2 are two different faces of any tetrahedron K with the same orientation, i.e., both pointing either inward or outward with respect to K. With this in mind, we now estimate Λ as follows:

$$\|\Lambda\|^2_{\boldsymbol{H}(\mathrm{div};K_1)} \le C\sum_{i=1}^{3}\|(\mathbf{b}_{f_i} - \mathbf{b}_f)\|^2_{\boldsymbol{L}^2(K_1)} \left(\int_{S_{e_i,\tilde{e}_i}} \mathbf{E}^1_{\mathrm{div}}\mathbf{u}\cdot\mathrm{d}\vec{S}\right)^2$$
$$\le C\sum_{i=1}^{3}\left(\|\mathbf{b}_{f_i}\|_{\boldsymbol{L}^2(K_1)} + \|\mathbf{b}_f\|^2_{\boldsymbol{L}^2(K_1)}\right)\left(\int_{S_{e_i,\tilde{e}_i}} \mathbf{E}^1_{\mathrm{div}}\mathbf{u}\cdot\mathrm{d}\vec{S}\right)^2$$
$$\le C\frac{|S_{e,\tilde{e}}|}{h}\left(\int_{S_{e,\tilde{e}}} |\mathbf{E}^1_{\mathrm{div}}\mathbf{u}|^2\,\mathrm{d}S\right)$$

where we employ the L^2-estimates for the basis function $\mathbf{b}_f$ $\mathbf{b}_{f_i}$ in Lemma 2.8 and use the Cauchy-Schwarz inequality in the last inequality.

It is pointed out that the local error estimate above is done within an element. The same argument can be applied for any element patch by combining K_1 with adjacent interface elements with no interface face of the first kind. Hence taking summation over all the interface faces and noticing that all slender volumes corresponding to the interface faces of the first kind are restricted in the δ-region with finite overlap due to the quasi-uniformity assumption of the triangulation, i.e.,

$$\bigcup_{\substack{f\in\mathcal{F}_h\\ f\subset S_\delta}} V_{f,\tilde{f}} \subset S_\delta\,, \tag{4.10}$$

thus we obtain

$$\begin{aligned}
&\sum_{K\in\mathcal{T}_*^1}\left\|\mathbf{\Pi}_h\mathbf{E}_{\mathrm{div}}^1\mathbf{u}-\widetilde{\mathbf{\Pi}}_h\mathbf{E}_{\mathrm{div}}^1\mathbf{u}\right\|_{\boldsymbol{H}(\mathrm{div};K)}^2\\
&\lesssim\sum_{K\in\mathcal{T}_*^1}\left(\sum_{\substack{f\in\mathcal{F}_h\\ f\subset\overline{K}\cap S_\delta}}\frac{|V_{f,\tilde{f}}|}{h^3}\left(\int_{V_{f,\tilde{f}}}|\operatorname{div}\mathbf{E}_{\mathrm{div}}^1\mathbf{u}|^2\,\mathrm{d}V\right)+\sum_{\substack{e\in\mathcal{E}_h\\ e\subset\overline{K}\cap S_\delta}}\frac{|S_{e,\tilde{e}}|}{h}\left(\int_{S_{e,\tilde{e}}}|\mathbf{E}_{\mathrm{div}}^1\mathbf{u}|^2\,\mathrm{d}S\right)\right)\\
&\lesssim\frac{\delta}{h}\left\|\operatorname{div}\mathbf{E}_{\mathrm{div}}^1\mathbf{u}\right\|_{\boldsymbol{L}^2(S_\delta)}^2+\frac{\delta}{h}\left\|\mathbf{E}_{\mathrm{div}}^1\mathbf{u}\right\|_{\boldsymbol{L}^2(S_\delta)}^2+\delta\left\|\mathbf{grad}\,\mathbf{E}_{\mathrm{div}}^1\mathbf{u}\right\|_{\boldsymbol{L}^2(S_\delta)}^2\\
&\lesssim(\frac{\delta^2}{h}+\delta)\left\|\mathbf{u}\right\|_{\boldsymbol{H}^1(\mathrm{div};\Omega_1)}^2.
\end{aligned}\tag{4.11}$$

Here we substitute (2.4) into the first inequality, make use of the inclusion (4.10) and apply Lemma 3.6 in the second one, and finally employ the δ-strip argument (Corollary 3.2) together with the continuity of the extension operator $\mathbf{E}_{\mathrm{div}}^1$ in the last one.

Now for any non-interface element $K\in\mathcal{T}^1$, $\mathbf{u}\in\boldsymbol{H}^1(\mathrm{div};K)$ and $\mathbf{u}-\widetilde{\mathbf{\Pi}}_h\mathbf{u}=\mathbf{u}-\mathbf{\Pi}_h\mathbf{u}$. Again a classical interpolation result (cf. [21]) yields

$$\begin{aligned}
\sum_{K\in\mathcal{T}^1}\left\|\mathbf{u}-\widetilde{\mathbf{\Pi}}_h\mathbf{u}\right\|_{\boldsymbol{H}(\mathrm{div};K)}^2&=\sum_{K\in\mathcal{T}^1}\left\|\mathbf{u}-\mathbf{\Pi}_h\mathbf{u}\right\|_{\boldsymbol{H}(\mathrm{div};K)}^2\\
\lesssim\sum_{K\in\mathcal{T}^1}h^2\left\|\mathbf{u}\right\|_{\boldsymbol{H}^1(\mathrm{div};K)}^2&\lesssim h^2\left\|\mathbf{u}\right\|_{\boldsymbol{H}^1(\mathrm{div};\Omega_1)}^2
\end{aligned}\tag{4.12}$$

Combining (4.6), (4.7), (4.8), (4.11), and (4.12) yields

$$\sum_{K\in\mathcal{T}^1\cup\mathcal{T}_*^1}\left\|\mathbf{u}-\widetilde{\mathbf{\Pi}}_h\mathbf{u}\right\|_{\boldsymbol{H}(\mathrm{div};K)}^2\lesssim(\frac{\delta^2}{h}+\delta+h^2)\left\|\mathbf{u}\right\|_{\boldsymbol{H}^1(\mathrm{div};\Omega_1)}^2\tag{4.13}$$

Completely analogously, we repeat the previous argument by interchanging the indices from 1 to 2 and arrive at the error estimate for any $K\in\mathcal{T}^2\cup\mathcal{T}_*^2$. The desired error estimate results from combining the two parts of contribution, which completes our proof.

□

Now we are in a position to state our main theorem about the optimal convergence of Galerkin solutions of $\boldsymbol{H}(\mathrm{div})$-elliptic interface problems by face elements.

Theorem 4.3. *Let* $\mathbf{u}$ *and* $\mathbf{u}_h$ *be the solutions to problems* $(\mathbf{Q})$ *and* $(\widetilde{\mathbf{Q}}_h)$*, respectively, and assume* $\mathbf{u}\in\boldsymbol{H}_0(\mathrm{div};\Omega)\cap\boldsymbol{H}^1(\mathrm{div};\Omega_1)\cap\boldsymbol{H}^1(\mathrm{div};\Omega_2)$*. Then we have the following error estimate under Assumptions 2.1 and 2.3:*

$$\left\|\mathbf{u}-\mathbf{u}_h\right\|_{\boldsymbol{H}(\mathrm{div};\Omega)}\leq Ch(\left\|\mathbf{u}\right\|_{\boldsymbol{H}^1(\mathrm{div};\Omega_1)}+\left\|\mathbf{u}\right\|_{\boldsymbol{H}^1(\mathrm{div};\Omega_2)})\tag{4.14}$$

with constant $C>0$ *depending on* χ_i*'s,* β_i*'s,* $\rho(\mathcal{T}_h)$*,* $\gamma(\mathcal{T}_h)$ *and* Ω*, but independent of* h*,* δ *and* $\mathbf{u}$*.*

Proof. We apply the first Strang lemma (see, e.g., [10], Theorem 4.1.1) to (2.9) and (2.11)

$$\left\|\mathbf{u}-\mathbf{u}_h\right\|_{\boldsymbol{H}(\mathrm{div};\Omega)}\leq C\inf_{\mathbf{w}_h\in\mathbf{F}_h}\left\{\left\|\mathbf{u}-\mathbf{w}_h\right\|_{\boldsymbol{H}(\mathrm{div};\Omega)}+\sup_{\mathbf{v}_h\in\mathbf{F}_h}\frac{|a(\mathbf{w}_h,\mathbf{v}_h)-a_h(\mathbf{w}_h,\mathbf{v}_h)|}{\left\|\mathbf{v}_h\right\|_{\boldsymbol{H}(\mathrm{div};\Omega)}}\right\}.\tag{4.15}$$

In particular, we choose $\mathbf{w}_h=\widetilde{\mathbf{\Pi}}_h\mathbf{u}$. By Lemma 4.2 we have

$$\left\|\mathbf{u}-\widetilde{\mathbf{\Pi}}_h\mathbf{u}\right\|_{\boldsymbol{H}(\mathrm{div};\Omega)}\leq C(\frac{\delta}{\sqrt{h}}+h+\sqrt{\delta})\left(\left\|\mathbf{u}\right\|_{\boldsymbol{H}^1(\mathrm{div};\Omega_1)}+\left\|\mathbf{u}\right\|_{\boldsymbol{H}^1(\mathrm{div};\Omega_2)}\right).\tag{4.16}$$

Next, for any $\mathbf{v}_h \in \mathbf{F}_h$ we can derive by using Lemma 4.1 and Corollary 3.2 that

$$\begin{aligned} |a^{\Delta}(\widetilde{\mathbf{\Pi}}_h\mathbf{u},\mathbf{v}_h)| &\leq C \quad \|\widetilde{\mathbf{\Pi}}_h\mathbf{u}\|_{\boldsymbol{H}(\mathrm{div};S_\delta)}\|\mathbf{v}_h\|_{\boldsymbol{H}(\mathrm{div};S_\delta)} \\ &\leq C \quad \left(\|\mathbf{u}\|_{\boldsymbol{H}(\mathrm{div};S_\delta)} + \|\mathbf{u}-\widetilde{\mathbf{\Pi}}_h\mathbf{u}\|_{\boldsymbol{H}(\mathrm{div};S_\delta)}\right)\|\mathbf{v}_h\|_{\boldsymbol{H}(\mathrm{div};S_\delta)} \\ &\leq C \quad (\sqrt{\delta}+h+\frac{\delta}{\sqrt{h}})\left(\|\mathbf{u}\|_{\boldsymbol{H}^1(\mathrm{div};\Omega_1)} + \|\mathbf{u}\|_{\boldsymbol{H}^1(\mathrm{div};\Omega_2)}\right)\|\mathbf{v}_h\|_{\boldsymbol{H}(\mathrm{div};\Omega)}\,, \end{aligned}$$

which implies that

$$\sup_{v\in\mathbf{F}_h}\frac{|a^{\Delta}(\widetilde{\mathbf{\Pi}}_h\mathbf{u},\mathbf{v}_h)|}{\|\mathbf{v}_h\|_{\boldsymbol{H}(\mathrm{div};\Omega)}} \leq C(\sqrt{\delta}+h+\frac{\delta}{\sqrt{h}})\left(\|\mathbf{u}\|_{\boldsymbol{H}^1(\mathrm{div};\Omega_1)} + \|\mathbf{u}\|_{\boldsymbol{H}^1(\mathrm{div};\Omega_2)}\right). \tag{4.17}$$

The desired estimate now follows from Assumption 2.3 by substituting $\delta \sim \mathscr{O}(h^2)$ into wherever δ occurs in (4.15)-(4.17) and plugging (4.16)-(4.17) into (4.15). □

Remark 4.4. *The optimal convergence result in Theorem 4.3 does not address the impact of coefficients, which is implicitly taken into account in the generic constant C. Actually the relative size ratio of coefficients could have enormous effect in the numerical computation, especially when it is extremely large or small. This issue is beyond the scope of our current work and will be addressed in the future.*

5 Numerical experiments

In this section, we conduct numerical test to verify the theoretical prediction of the convergence analysis developed in previous sections. Our numerical experiments are implemented using MATLAB combined with the commercial package FEMLAB. We will test the first family of Nédélec face elements of the lowest order. It is remarked that we use non-nested families of triangulations in order to make sure they are interface-aware. Note that after each step of mesh refinement, some regularly refined interface elements have to be slightly adjusted to meet the interface-aware condition.In the sequel, we will test the convergence rates for the relative error in the $\boldsymbol{H}(\mathrm{div};\Omega)$-norm which is defined by

$$\text{Relative } \boldsymbol{H}(\mathrm{div};\Omega) \text{ error} := \frac{\|\mathbf{u}-\mathbf{u}_h\|_{\boldsymbol{H}(\mathrm{div};\Omega)}}{\|\mathbf{u}\|_{\boldsymbol{H}(\mathrm{div};\Omega)}}, \tag{5.1}$$

and relative error in the energy norm, namely,

$$\text{Relative energy error} := \frac{\|\mathbf{u}-\mathbf{u}_h\|_a}{\|\mathbf{u}\|_a}. \tag{5.2}$$

Note that both $\boldsymbol{H}(\mathrm{div};\Omega)$ and energy norms are numerically computed using a fourth order quadrature rule.

Example 5.1. The computational domain is taken to be a ball $\Omega = \{(x,y,z);\ x^2+y^2+z^2 \leq r_2\}$, and the interface Γ is a spherical surface $\{(x,y,z);\ x^2+y^2+z^2 = r_1\}$. The exact solution $\mathbf{u}(x,y,z)$ is given by

$$\mathbf{u}(x,y,z) = \begin{cases} \dfrac{1}{\chi_1}\mathbf{u}_1(x,y,z), & \text{if } x^2+y^2+z^2 \leq r_1\,; \\ \dfrac{1}{\chi_2}\mathbf{u}_2(x,y,z), & \text{if } r_1 < x^2+y^2+z^2 \leq r_2\,, \end{cases} \tag{5.3}$$

where $\mathbf{u}_1(x,y,z)$ is given by

$$\begin{pmatrix} (y-z)+n_1(r_1^2-x^2-y^2)(z-x)-n_1(r_1^2-x^2-y^2)(x-y) \\ -n_1(r_1^2-x^2-y^2)(y-z)+(z-x)+n_1(r_1^2-x^2-y^2)(x-y) \\ n_1(r_1^2-x^2-y^2)(y-z)-n_1(r_1^2-x^2-y^2)(z-x)+(x-y) \end{pmatrix}$$

and $\mathbf{u}_2(x,y,z)$ by

$$\begin{pmatrix} (y-z)+n_2(r_1^2-x^2-y^2)(r_2^2-x^2-y^2)(z-x)-n_2(r_1^2-x^2-y^2)(r_2^2-x^2-y^2)(x-y) \\ -n_2(r_1^2-x^2-y^2)(r_2^2-x^2-y^2)(y-z)+(z-x)+n_2(r_1^2-x^2-y^2)(r_2^2-x^2-y^2)(x-y) \\ n_2(r_1^2-x^2-y^2)(r_2^2-x^2-y^2)(y-z)-n_2(r_1^2-x^2-y^2)(r_2^2-x^2-y^2)(z-x)+(x-y) \end{pmatrix}$$

For this example, we fix $r_1 = 1$, $r_2 = 2$, $n_2 = 20$, $n_1 = n_2(r_2^2 - r_1^2)$, $\beta_1 = \beta_2 = 1$ and derive the source functions $\mathbf{f}$ through the equation (1.1) for different pairs of χ_1 and χ_2, using the exact solution (5.3) which satisfies the homogeneous boundary condition and jump conditions on the interface. Numerical convergence tests are carried out to analyze the rates of the error decay using lowest order face elements of the first family. We start our tests on a rather coarse mesh with maximun mesh size $h = 2$ and then refine the mesh in a regular and uniform way which subdivides a coarse element into eight smaller ones. The refinement process will be done for three consecutive times which amounts to $2,568,192$ degrees of freedom at the finest mesh with mesh size $h = 0.125$.

A slice view of the interface-aware mesh are shown in Figure 7 (a). From Figure 7 (b) with $\chi_1 = 1$ and $\chi_2 = 10$, it can be clearly seen that as the mesh gets finer and finer, the line of the convergence rate tends to be parallel to the reference line of first order convergence in terms of the mesh size. More precisely, in the asymptotic sense, face elements indeed yield the optimal first order convergence in the $\boldsymbol{H}(\mathrm{div};\Omega)$ norm as predicted by theory. Next, we adjust the relative jump of the coefficients χ_2/χ_1 to be 10^3 and 10^{-3}, respectively, and also plot the corresponding convergence rates in Figure 7 (c) and Figure 7 (d). Similar observations with asymptotic tendency of first order convergence rate with respect to the meshsize further consolidate our theoretical result.

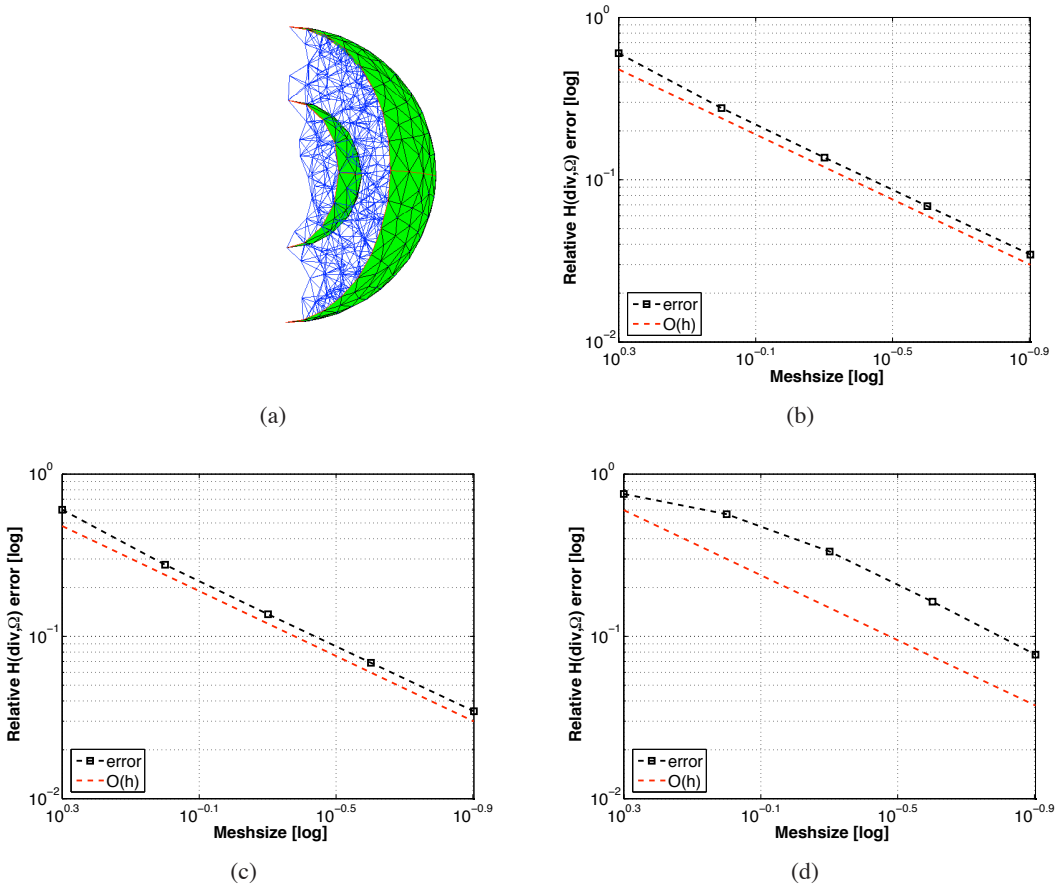

Figure 7: (a): A sample slice view of the triangulation of interface-aware mesh in 3D; (b): The convergence rate when $\chi_1 = 1, \chi_2 = 10$; (c): The convergence rate when $\chi_1 = 1, \chi_2 = 10^3$; (d): The convergence rate when $\chi_1 = 1, \chi_2 = 10^{-3}$.

Last, we test the relation between the relative error in the energy norm and relative jump of the coefficients χ_2/χ_1. On a typical fine mesh with mesh size $h = 0.1232$ with 4,396,225 degrees of freedom. We increase the relative jump of coefficients from 10^{-8} to 10^{8} by fixing χ_1 or χ_2 to be unity and plot the corresponding relative energy error curve versus the relative jump in Figure 8, It can be seen that the numerical solution converges quite robustly in the sense of energy norm with respect to the relative jump of coefficients.

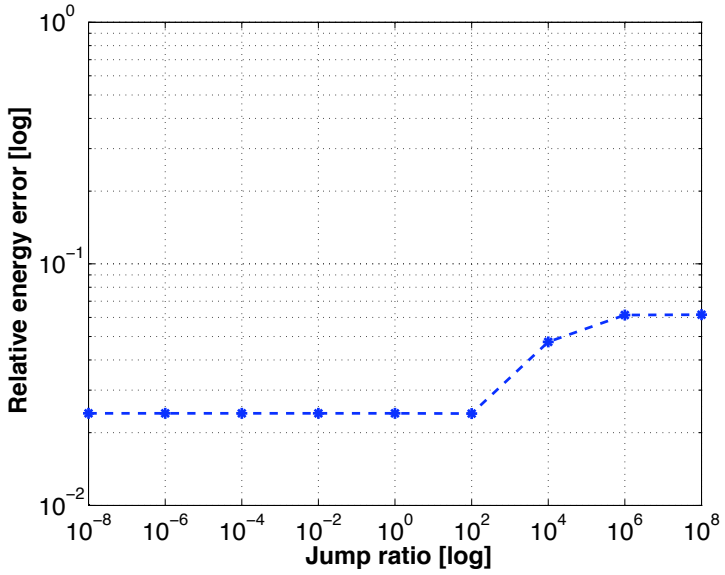

Figure 8: Relative error in the energy norm versus relative jump of coefficients for a fine triangulation with meshsize $h = 0.1232$ in Example 5.1.

6 Conclusion

We have analyzed the convergence of the $\boldsymbol{H}(\mathrm{div};\Omega)$-conforming finite element method for $\boldsymbol{H}(\mathrm{div};\Omega)$-elliptic interface problems based on families of interface-aligned meshes. The difficulty mainly arises from the discontinuity of the coefficient in the second order term of equation (1.1). Optimal convergence results in $\boldsymbol{H}(\mathrm{div};\Omega)$-norm are obtained under reasonable regularity assumptions. With this work, we have completed the finite element convergence analysis for standard second order elliptic interface problems [19], $\boldsymbol{H}(\mathbf{curl};\Omega)$-elliptic interface problems [16] and $\boldsymbol{H}(\mathrm{div};\Omega)$-elliptic interface problems (this work). Optimal rates can be established for each case.

A Appendix

Proof of Theorem 3.4. 1. We first prove the half ball extension following [1,25].

For a fixed $\mathbf{x}^0 \in \Gamma$, we first suppose that ∂U is flat near $\mathbf{x}^0$ which is lying in the plane $\{\mathbf{x} \mid x_3 = 0\}$. We assume that there exists an open ball $B = \{\mathbf{x}; |\mathbf{x} - \mathbf{x}^0| < r\}$ with center $\mathbf{x}^0$ and radius $r > 0$ such that

$$\begin{cases} B^+ := B \cap \{x_3 \geq 0\} \subset \overline{U}, \\ B^- := B \cap \{x_3 < 0\} \subset \mathbb{R}^3 \setminus \overline{U}. \end{cases}$$

2. Suppose $\mathbf{p} \in \boldsymbol{C}^\infty(\overline{U})$. We define a $\boldsymbol{H}^1(\mathbf{curl})$ reflection of $\mathbf{p}$ from B^+ to B^-.

$$\widetilde{\mathbf{p}} = \begin{cases} \mathbf{p}(\mathbf{x}), & \text{if } \mathbf{x} \in B^+; \\ \begin{pmatrix} \sum_{j=1}^3 \lambda_j p^1(x_1, x_2, -\frac{x_3}{j}) \\ \sum_{j=1}^3 \lambda_j p^2(x_1, x_2, -\frac{x_3}{j}) \\ \sum_{j=1}^3 -\frac{\lambda_j}{j} p^3(x_1, x_2, -\frac{x_3}{j}) \end{pmatrix}, & \text{if } \mathbf{x} \in B^-. \end{cases} \tag{A.1}$$

where $(\lambda_1, \lambda_2, \lambda_3)$ are the unique solutions of the 3×3 system of linear equations

$$\sum_{j=1}^3 (-\frac{1}{j})^k \lambda_j = 1, \quad k = 0, 1, 2, \tag{A.2}$$

which has the unique solution $(\lambda_1, \lambda_2, \lambda_3) = (6, -32, 27)$. It is readily checked that

$$\widetilde{\mathbf{p}} \in \boldsymbol{C}^1(\overline{B}).$$

Now we define a reflection of $\mathbf{curl}\,\mathbf{p}$ from B^+ to B^- in view of (3.3).

$$\widetilde{\mathbf{curl}\,\mathbf{p}} = \begin{cases} \mathbf{curl}\,\mathbf{p}, & \text{if } \mathbf{x} \in B^+; \\ \mathbf{curl}\,\widetilde{\mathbf{p}}, & \text{if } \mathbf{x} \in B^-, \end{cases} \tag{A.3}$$

or

$$\widetilde{\mathbf{curl}\,\mathbf{p}} = \begin{cases} \begin{pmatrix} p^3_{x_2} - p^2_{x_3} \\ p^1_{x_3} - p^3_{x_1} \\ p^2_{x_1} - p^1_{x_2} \end{pmatrix}, & \text{if } \mathbf{x} \in B^+; \\ \begin{pmatrix} \sum_{j=1}^3 -\frac{\lambda_j}{j} p^3_{x_2}(x_1, x_2, -\frac{x_3}{j}) - \sum_{j=1}^3 -\frac{\lambda_j}{j} p^2_{x_3}(x_1, x_2, -\frac{x_3}{j}) \\ \sum_{j=1}^3 -\frac{\lambda_j}{j} p^1_{x_3}(x_1, x_2, -\frac{x_3}{j}) - \sum_{j=1}^3 -\frac{\lambda_j}{j} p^3_{x_1}(x_1, x_2, -\frac{x_3}{j}) \\ \sum_{j=1}^3 \lambda_j p^2_{x_1}(x_1, x_2, -\frac{x_3}{j}) - \sum_{j=1}^3 \lambda_j p^1_{x_2}(x_1, x_2, -\frac{x_3}{j}) \end{pmatrix}, & \text{if } \mathbf{x} \in B^-. \end{cases} \tag{A.4}$$

Comparing the components of $\widetilde{\mathbf{curl}\,\mathbf{p}}$ in (A.4) in B^+ and B^-, we derive a tentative extension formula for a vector-valued function $\mathbf{w} = (w_1, w_2, w_3)^t \in \boldsymbol{C}^\infty(B^+)$ as follows:

$$\widetilde{\mathbf{w}}(\mathbf{x}) = \begin{pmatrix} \widetilde{w^1}(\mathbf{x}) \\ \widetilde{w^2}(\mathbf{x}) \\ \widetilde{w^3}(\mathbf{x}) \end{pmatrix} := \begin{cases} \mathbf{w}(\mathbf{x}), & \text{if } \mathbf{x} \in B^+; \\ \begin{pmatrix} \sum_{j=1}^3 -\frac{\lambda_j}{j} w^1(x_1, x_2, -\frac{x_3}{j}) \\ \sum_{j=1}^3 -\frac{\lambda_j}{j} w^2(x_1, x_2, -\frac{x_3}{j}) \\ \sum_{j=1}^3 \lambda_j w^3(x_1, x_2, -\frac{x_3}{j}) \end{pmatrix}, & \text{if } \mathbf{x} \in B^-. \end{cases} \tag{A.5}$$

3. We claim $\widetilde{\mathbf{w}} \in \boldsymbol{C}^1(B)$ and thus $\operatorname{div} \widetilde{\mathbf{w}} \in C^0(B)$. This can be demonstrated by a detailed computation. Indeed according to (A.5) and (A.2),

$$\lim_{x_3 \to 0+} \widetilde{w^i}(\mathbf{x}) = \lim_{x_3 \to 0-} \widetilde{w^i}(\mathbf{x}) \qquad i = 1, 2, 3, \tag{A.6}$$

$$\lim_{x_3 \to 0+} \widetilde{w^i}_{x_j}(\mathbf{x}) = \lim_{x_3 \to 0-} \widetilde{w^i}_{x_j}(\mathbf{x}) \quad i, j = 1, 2, 3. \tag{A.7}$$

4. We prove

$$\|\widetilde{\mathbf{w}}\|_{\boldsymbol{H}^1(\mathrm{div};B)} \le C\,\|\mathbf{w}\|_{\boldsymbol{H}^1(\mathrm{div};B^+)}\ . \tag{A.8}$$

In fact, by the definition of $\widetilde{\mathbf{w}}$ we can derive

$$\begin{aligned}
&\int_B |\widetilde{\mathbf{w}}(\mathbf{x})|^2\,\mathrm{d}\mathbf{x} = \int_{B^+} |\mathbf{w}(\mathbf{x})|^2\,\mathrm{d}\mathbf{x} + \int_{B^-} |\sum\nolimits_{j=1}^3 \frac{\lambda_j}{-j} w^1(x_1,x_2,-\frac{x_3}{j})|^2\,\mathrm{d}\mathbf{x}\\
&+\int_{B^-} |\sum\nolimits_{j=1}^3 \frac{\lambda_j}{-j} w^2(x_1,x_2,-\frac{x_3}{j})|^2\,\mathrm{d}\mathbf{x} + \int_{B^-} |\sum\nolimits_{j=1}^3 \lambda_j w^3(x_1,x_2,-\frac{x_3}{j})|^2\,\mathrm{d}\mathbf{x}\\
&\le C\int_{B^+} |\mathbf{w}(\mathbf{x})|^2\,\mathrm{d}\mathbf{x}\ ,\\
&\int_B |\,\mathbf{grad}\,\widetilde{\mathbf{w}}(\mathbf{x})|^2\,\mathrm{d}\mathbf{x}\\
&=\sum_{i=1}^3\sum_{k=1}^3\int_{B^+} |w^i_{x_k}(\mathbf{x})|^2\,\mathrm{d}\mathbf{x} + \sum_{k=1}^3\int_{B^-} |\sum\nolimits_{j=1}^3 \frac{\lambda_j}{-j} w^1_{x_k}(x_1,x_2,-\frac{x_3}{j})|^2\,\mathrm{d}\mathbf{x}\\
&+\sum_{k=1}^3\int_{B^-} |\sum\nolimits_{j=1}^3 \frac{\lambda_j}{-j} w^2_{x_k}(x_1,x_2,-\frac{x_3}{j})|^2\,\mathrm{d}\mathbf{x} + \sum_{k=1}^3\int_{B^-} |\sum\nolimits_{j=1}^3 \lambda_j w^3_{x_k}(x_1,x_2,-\frac{x_3}{j})|^2\,\mathrm{d}\mathbf{x}\\
&\le C\int_{B^+} |\,\mathbf{grad}\,\mathbf{w}(\mathbf{x})|^2\,\mathrm{d}\mathbf{x}\ ,\\
&\int_B |\,\mathrm{div}\,\widetilde{\mathbf{w}}(\mathbf{x})|^2\,\mathrm{d}\mathbf{x} = \int_{B^+} |w^1_{x_1}(\mathbf{x}) + w^2_{x_2}(\mathbf{x}) + w^3_{x_3}(\mathbf{x})|^2\,\mathrm{d}\mathbf{x}\\
&+\int_{B^-} |\sum\nolimits_{j=1}^3 \frac{\lambda_j}{-j} w^1_{x_1}(x_1,x_2,-\frac{x_3}{j}) + \sum\nolimits_{j=1}^3 \frac{\lambda_j}{-j} w^2_{x_2}(x_1,x_2,-\frac{x_3}{j})\\
&+\sum\nolimits_{j=1}^3 \frac{\lambda_j}{-j} w^3_{x_3}(x_1,x_2,-\frac{x_3}{j})|^2\,\mathrm{d}\mathbf{x}\\
&\le C\int_{B^+} |\,\mathrm{div}\,\mathbf{w}(\mathbf{x})|^2\,\mathrm{d}\mathbf{x}\ ,\\
&\int_B |\,\mathbf{grad}\,\mathrm{div}\,\widetilde{\mathbf{w}}(\mathbf{x})|^2\,\mathrm{d}\mathbf{x}\\
&=\sum_{k=1}^3\int_{B^+} |w^1_{x_1,x_k}(\mathbf{x}) + w^2_{x_2,x_k}(\mathbf{x}) + w^3_{x_3,x_k}(\mathbf{x})|^2\,\mathrm{d}\mathbf{x}\\
&+\sum_{k=1}^3\int_{B^-} |\sum\nolimits_{j=1}^3 \frac{\lambda_j}{-j} w^1_{x_1,x_k}(x_1,x_2,-\frac{x_3}{j^{\lfloor (k+1)/2\rfloor}}) + \sum\nolimits_{j=1}^3 \frac{\lambda_j}{-j} w^2_{x_2,x_k}(x_1,x_2,-\frac{x_3}{j^{\lfloor (k+1)/2\rfloor}})\\
&+\sum\nolimits_{j=1}^3 \frac{\lambda_j}{-j} w^3_{x_3,x_k}(x_1,x_2,-\frac{x_3}{j^{\lfloor (k+1)/2\rfloor}})|^2\,\mathrm{d}\mathbf{x}\\
&\le C\int_{B^+} |\,\mathbf{grad}\,\mathrm{div}\,\mathbf{w}(\mathbf{x})|^2\,\mathrm{d}\mathbf{x}\ .
\end{aligned}$$

The estimate (A.8) now follows readily from the above four inequalities.

5. If ∂U is not flat near $\mathbf{x}^0$, we can find a C^2-mapping $\boldsymbol{\Phi}$, with the inverse $\boldsymbol{\Phi}^{-1}$, such that $\boldsymbol{\Phi}$ *flattens* ∂U near $\mathbf{x}^0$. We can write $\mathbf{y} = \boldsymbol{\Phi}(\mathbf{x})$, $\mathbf{x} = \boldsymbol{\Phi}^{-1}(\mathbf{y})$, and $\mathbf{v}(\mathbf{y}) := \mathbf{w}(\boldsymbol{\Phi}^{-1}(\mathbf{y}))$. Choosing a small ball B and arguing as in the previous steps, we can extend $\mathbf{v}$ from B^+ to a function $\widetilde{\mathbf{v}}$ defined in B such that $\widetilde{\mathbf{v}} \in \boldsymbol{C}^1(B)$ and thus $\mathbf{curl}\,\widetilde{\mathbf{v}} \in \boldsymbol{C}^0(B)$ and the following estimate holds for any $\mathbf{v} \in \boldsymbol{H}^1(\mathrm{div};B^+)$,

$$\|\widetilde{\mathbf{v}}\|_{\boldsymbol{H}^1(\mathrm{div};B)} \le C\,\|\mathbf{v}\|_{\boldsymbol{H}^1(\mathrm{div};B^+)}\ . \tag{A.9}$$

Letting $W := \boldsymbol{\Phi}^{-1}(B)$, $W^+ := \boldsymbol{\Phi}^{-1}(B^+)$ and converting back to the $\mathbf{x}$-variable, we have

$$\|\widetilde{\mathbf{v}}\|_{\boldsymbol{H}^1(\mathrm{div};W)} \le C\,\|\mathbf{v}\|_{\boldsymbol{H}^1(\mathrm{div};W^+)}\,. \tag{A.10}$$

6. Due to the compactness of ∂U, there exist finitely many open balls W_i, $i = 1, 2, \ldots, N$ such that $\partial U \subset \bigcup_{i=1}^{N} W_i$. Take $W_0 \subset\subset U$ such that $U \subset \bigcup_{i=0}^{N} W_i$. Let $\{\theta_i\}_{i=0}^{N}$ be a partition of unity associated with W_i, $i = 0, 1, 2, \ldots, N$. For any given smooth $\mathbf{w} = \sum_{i=0}^{N} \mathbf{w}_i$ with $\mathbf{w}_i = \theta_i \mathbf{w}$, let $\widetilde{\mathbf{w}} = \mathbf{w}_0 + \sum_{i=1}^{N} \widetilde{\mathbf{w}_i}$, where $\widetilde{\mathbf{w}_i}$ are extensions of $\mathbf{w}_i$ defined in W_i for $i = 1, 2, \ldots, N$. Replacing $\widetilde{\mathbf{v}}$ and $\mathbf{v}$ in (A.10) with $\widetilde{\mathbf{w}_i}$ and $\mathbf{w}_i$, respectively, and taking summation from 0 to N we obtain

$$\|\widetilde{\mathbf{w}}\|_{\boldsymbol{H}^1(\mathrm{div};\mathbb{R}^3)} \leq C \|\mathbf{w}\|_{\boldsymbol{H}^1(\mathrm{div};U)} . \tag{A.11}$$

for some constant C depending on U but not on $\mathbf{w}$.

7. Hereafter we define an extension operator

$$\mathbf{E}_{\mathrm{div}} \mathbf{w} = \widetilde{\mathbf{w}}$$

and observe that the mapping $\mathbf{w} \mapsto \mathbf{E}_{\mathrm{div}} \mathbf{w}$ is linear. Using the density of $\boldsymbol{C}^{\infty}(\overline{U})$ in $\boldsymbol{H}^1(\mathrm{div}; U)$, we can verify that the operator $\mathbf{E}_{\mathrm{div}}$ is what we desire.

□

References

[1] R. A. ADAMS, *Sobolev Spaces*, Academic Press, New York-London, 1975.

[2] D. N. ARNOLD, R. S. FALK, AND R. WINTHER, *Preconditioning in H(div) and applications*, Math. Comput., 66 (1997), pp. 957–984.

[3] J. W. BARRETT AND C. M. ELLIOTT, *Fitted and unfitted finite-element methods for elliptic equations with smooth interfaces*, IMA J. Numer. Anal., 7 (1987), pp. 283–300.

[4] J. H. BRAMBLE AND J. T. KING., *A finite element method for interface problems in domains with smooth boundaries and interfaces*, Adv. Comput. Math., 6 (1996), pp. 109–138.

[5] F. BREZZI AND M. FORTIN, *Mixed and Hybrid Finite Element Methods*, Springer-Verlag, New York, 1991.

[6] E. BURMAN AND P. HANSBO, *Interior penalty stabilized lagrange multiplier methods for the finite element solution of elliptic interface problems*, IMA Numer. Anal., accepted.

[7] Z. CAI, R. LAZAROV, T. MANTEUFFEL, AND S. MCCORMICK, *First-order system least-squares for partial differential equations: Part I*, SIAM J. Numer. Anal., 31 (1994), p. 1785–1799.

[8] T. CHAN AND J. ZOU, *A convergence theory of multilevel additive Schwarz methods on unstructured meshes*, Numerical Algorithms, 13 (1996), pp. 365–398.

[9] Z. CHEN AND J. ZOU, *Finite element methods and their convergence for elliptic and parabolic interface problems*, Numer. Math., 79 (1998), pp. 175–202.

[10] P. G. CIARLET, *The Finite Element Method for Elliptic Problems*, Studies in Mathematics and its Applications, North-Holland Pub. Co., Amsterdam, New York, 1 ed., 1978.

[11] L. C. EVANS, *Partial Differential Equations*, Providence, Rhode Island : American Mathematical Society, 1998.

[12] V. GIRAULT AND P. RAVIART, *Finite Element Methods for Navier-Stokes equations*, Springer, Berlin, 1986.

[13] A. HANSBO AND P. HANSBO, *An unfitted finite element method, based on Nitsche's method, for elliptic interface problems*, Comput. Methods Appl. Mech. Eng., 191 (2002), pp. 5537–5552.

[14] R. HIPTMAIR, *Multigrid method for H(div) in three dimensions*, Electron. Trans. Numer. Anal., 6 (1997), pp. 133–152.

[15] R. HIPTMAIR, *Finite elements in computational electromagnetism*, Acta Numerica, 11 (2002), pp. 237–339.

[16] R. HIPTMAIR, J.-Z. LI, AND J. ZOU, *Convergence analysis of finite element methods for H(curl)-elliptic interface problems*, Report 2009-04, SAM, ETH, Zürich, Switzerland, January 2009.

[17] R. HIPTMAIR AND J. XU, *Nodal auxiliary space preconditioning in H(curl) and H(div) spaces*, SIAM J. Numer. Anal., 45 (2007), pp. 2483–2509.

[18] J. HUANG AND J. ZOU, *A mortar element method for elliptic problems with discontinuous coefficients*, IMA J. Numer. Anal., 22 (2002), pp. 549–576.

[19] J. LI, J. M. MELENK, B. WOHLMUTH, AND J. ZOU, *Optimal a priori estimates for higher order finite elements for elliptic interface problems*, Appl. Numer. Math., (2009).

[20] Z. LI AND K. ITO, *The Immersed Interface Method : Numerical Solutions of PDEs Involving Interfaces and Irregular Domains*, Philadelphia : SIAM, 2006.

[21] P. MONK, *Finite Element Methods for Maxwell's Equations*, Clarendon Press, Oxford, 2003.

[22] J. NÉDÉLEC, *Mixed finite elements in* $\mathbb{R}^3$, Numer. Math., 35 (1980), pp. 315–341.

[23] P.-O. PERSSON AND G. STRANG, *A simple mesh generator in matlab*, SIAM Review, 46 (2004), pp. 329–345.

[24] M. PLUM AND C. WIENERS, *Optimal a priori estimates for interface problems*, Numer. Math., 95 (2003), pp. 735–759.

[25] S. SEELEY, *Extensions of* C^∞ *functions defined on a half space*, Proc. Amer. Math. Soc., 15 (1961), pp. 625–626.

[26] P. VASSILEVSKI AND R. LAZAROV, *Preconditioned mixed finite element saddle point elliptic problems*, Numer. Lin. Alg. Appl., 3 (1996), pp. 1–20.

Research Reports

No.	Authors/Title
10-14	*R. Hiptmair, J. Li and J. Zou* Convergence analysis of Finite Element Methods for $H(\mathrm{div};\Omega)$-elliptic interface problems
10-13	*M.H. Gutknecht and J.-P.M. Zemke* Eigenvalue computations based on IDR
10-12	*H. Brandsmeier, K. Schmidt and Ch. Schwab* A multiscale hp-FEM for 2D photonic crystal band
10-11	*V.H. Hoang and C. Schwab* Sparse tensor Galerkin discretizations for parametric and random parabolic PDEs. I: Analytic regularity and gpc-approximation
10-10	*V. Gradinaru, G.A. Hagedorn, A. Joye* Exponentially accurate semiclassical tunneling wave functions in one dimension
10-09	*B. Pentenrieder and C. Schwab* *hp*-FEM for second moments of elliptic PDEs with stochastic data. Part 2: Exponential convergence
10-08	*B. Pentenrieder and C. Schwab* *hp*-FEM for second moments of elliptic PDEs with stochastic data. Part 1: Analytic regularity
10-07	*C. Jerez-Hanckes and J.-C. Nédélec* Asymptotics for Helmholtz and Maxwell solutions in 3-D open waveguides
10-06	*C. Schwab and O. Reichmann* Numerical analysis of additive, Lévy and Feller processes with applications to option pricing
10-05	*C. Schwab and R. Stevenson* Fast evaluation of nonlinear functionals of tensor product wavelet expansions
10-04	*B.N. Khoromskij and C. Schwab* Tensor-structured Galerkin approximation of parametric and stochastic elliptic PDEs
10-03	*A. Cohen, R. DeVore and C. Schwab* Analytic regularity and polynomial approximation of parametric and stochastic elliptic PDEs